

DIPLOMARBEIT

Analysis of anti-islanding protection methods for inverter connected DER

Ausgeführt zum Zwecke der Erlangung des akademischen Grades eines

Diplom-Ingenieurs (Dipl.-Ing.)

unter der Leitung von

Univ.-Prof. Dr.-Ing. Wolfgang Gawlik

und

Dipl.-Ing. Dominik Fasthuber

Institut für Energiesysteme und Elektrische Antriebe

eingereicht an der

Technischen Universität Wien

Fakultät für Elektrotechnik und Informationstechnik

von

Klemen Peter Kosovinc BSc

1527844

Lerchengasse 7

1080 Wien

Wien, im September 2017

Arbeitsgruppe für Elektrische Anlagen

A-1040 Wien, Gusshausstr. 25, Internet: <http://www.ea.tuwien.ac.at>

Acknowledgements

I would like to thank my mentor Univ.Prof. Dr.-Ing. Gawlik Wolfgang and co-mentor Dipl.-Ing. Fasthuber Dominik for their help and directions during the work on my master thesis. Furthermore, I would like to thank Technische Universität Wien for the knowledge I gained and especially for the way I was treated there as a foreigner.

I am also sincerely thankful to the people closest to me, who showed me their support throughout the study.

Kurzfassung

Der Klimawandel und das Strommarktwachstum führen im 21. Jahrhundert zu vielen Herausforderungen für das Stromnetz. Eines von vielen problematischen Fragen ist das enorme anwachsen von Umrichter basierten DEGs, welche potentiell gefährlich für eine ungewollte Inselnetzbildung sind. Verschiedene Methoden zur Detektion ungewollter Inselnetze können in Kombination mit verschiedenen Umrichterregelungen den Bereich der Non Detection Zone (NDZ) beeinflussen. Daher wurden über/unter Spannungs- und Frequenzschutz in Kombination mit $P(U)$, $Q(U)$ und $\cos\varphi(U)$ Umrichterregelungen erforscht. Ziel war es, die erworbenen NDZs zu beobachten und den Kompromiss im technischen und ökonomischen Sinne zu finden, um einen ordnungsgemäßen Schutz vor einer Inselbildung zu gewährleisten.

Ein Analytischer Ansatz für die NDZ-Berechnung zeigte, dass die Spannungsschutzgrenzen vor allem durch die aktive Leistungsfehlانpassung zwischen Last und DEG beeinflusst werden, während Frequenzschutzgrenzen durch Blindleistungsfehlانpassung beeinflusst werden. Es wurde ein Simulationsmodell in Matlab Simulink gebaut und Lastcharakteristiken variiert, um verschiedene Leistungsfehlانpassungen zwischen Last und DEG zu testen. Der Simulationsverlauf des Modells wurde in zwei Phasen aufgeteilt: Ein Netzbetrieb, bei dem Frequenz und Spannung durch das Netz beeinflusst wird und ein Inselbetrieb, der durch die Leistungsfehlانpassung zwischen Last und DEG beeinflusst wird.

Der Vergleich von analytischen und simulierten NDZs zeigte wesentliche Unterschiede welche nicht durch die analytische Berechnung alleine gezeigt werden konnten. Besonders das dynamische Verhalten von Spannung und Frequenz nach dem Übergang vom Netz zum Inselbetrieb wurde nicht berücksichtigt. Genau dieses Verhalten zeigte die Einführung der neuen Methode zur Detektion ungewollter Inselnetze: Rate Of Change Of Frequency (ROCOF).

Die $Q(U)$ Umrichterregelung erwies sich als die beste unter den recherchierten Regelun-

Kurzfassung

gen in Bezug auf die Größe der NDZ, Blindleistungsunterstützung und im ökonomischen Sinne. Die Ergänzung der selbst implementierten ROCOF-Schutzmethode hat auch bewiesen, dass die Größe des NDZ-Bereichs der $Q(U)$ Regelung weiter reduziert werden kann.

Abstract

Climate changes and electricity market growth are creating a lot of challenges for power grid in the 21st century. One among many problematic issues is also huge growth of inverter connected Distributed Energy Generation (DEG), which is potentially dangerous for unwanted islanding. Different anti-islanding protection methods can in combination with different inverter regulations influence the area of Non Detection Zone (NDZ). Over/under voltage and frequency protection anti-islanding functions were therefore researched in combination with $P(U)$, $Q(U)$ and $\cos\varphi(U)$ inverter regulations. The goal was to observe the acquired NDZs and to find the best compromise in technical and economical sense in order to ensure proper protection against islanding.

Analytical approach for NDZ calculation showed, that voltage protection borders are mainly influenced with active power mismatch between load and DEG, while frequency protection limits are influenced with reactive power mismatch. Simulation model was built in Matlab Simulink and load characteristics were changed in order to test different power mismatches between load and DEG. Simulation course of the model was separated in two phases: grid mode, where frequency and voltage were influenced by grid and island mode, where they were influenced by the power mismatch between load and DEG.

Comparison of analytical and simulated NDZs offered the insight, on which characteristics could not be acquired with analytical calculation. Especially dynamic behaviour of voltage and frequency after the transition from grid to island mode were not taken into account. This behaviour offered the introduction of new anti-islanding protection method to the model: Rate Of Change Of Frequency (ROCOF).

$Q(U)$ inverter regulation proved to be the best among researched regulations in terms of the size of the NDZ, reactive power support to the grid and in economical sense. Addition of self-implemented ROCOF protection method also proved, that size of the NDZ area of $Q(U)$ regulation can be further reduced.

Contents

Kurzfassung	iii
Abstract	v
1 Introduction	1
1.1 Islanding operation - definition	2
1.2 Structure of the thesis	4
2 State of the art	7
2.1 Theoretical findings	7
2.2 Thesis's conclusion	11
2.3 Further work	11
3 Theoretical background	15
3.1 Dispersed generation problem in context with islanding	15
3.2 Requirements for connection of inverter connected DER on the grid	16
3.2.1 Behaviour of inverter connected generation units on distribution grid	17
3.2.2 Inverter regulation strategies	17
3.2.3 Protection for decoupling point	22
3.3 Protection methods	22
3.4 Passive Methods	23
3.4.1 Over/under voltage and over/under frequency protection method . .	23
3.4.2 Phase jump detection method	24
3.4.3 Detection of harmonics	25
3.4.4 Rate of change of frequency (ROCOF)	26
3.4.5 Other passive methods	28

4 Analytical background	31
4.1 MATLAB Simulink model	31
4.1.1 Basic description	31
4.1.2 Protection settings	34
4.1.3 Plotting of the NDZ	34
4.1.4 Inverter regulation setting	35
4.2 Analytical calculation of NDZs	38
4.2.1 $P(U)$ inverter regulation	39
4.2.2 $P(U) + \text{constant } \cos\varphi_{PV} = 0.925 \text{ over excited}$ inverter regulation . .	42
4.2.3 $Q(U)$ inverter regulation	45
4.2.4 $\cos\varphi(U)$ inverter regulation	48
5 Results and analysis	55
5.1 The course of simulation	55
5.2 Simulated NDZs	58
5.2.1 $P(U)$ inverter regulation	58
5.2.2 $P(U) + \text{constant } \cos\varphi_{PV} = 0.925 \text{ over excited}$ inverter regulation .	61
5.2.3 $Q(U)$ inverter regulation	62
5.2.4 $\cos\varphi(U)$ inverter regulation	64
5.3 Transition from grid mode to island mode	66
5.3.1 $P(U)$ inverter regulation	66
5.3.2 $P(U) + \text{constant } \cos\varphi_{PV} = 0.925 \text{ over excited}$ inverter regulation .	69
5.3.3 $Q(U)$ inverter regulation	71
5.3.4 $\cos\varphi(U)$ inverter regulation	73
5.4 Simulink model's efficiency	73
5.5 Further research of $Q(U)$ inverter regulation	75
5.5.1 $Q(U)$ inverter regulation with ROCOF	77
5.5.2 $Q(U)$ and $P(f)$ inverter regulation	78
5.5.3 $Q(U)$ and $P(f)$ inverter regulation with ROCOF	80
6 Conclusion and future work	81
Bibliography	87

1 Introduction

Modern power system is experiencing huge growth of Distributed Energy Generation (DEG) in the 21st century [1]. In year 2007, European Union (EU) introduced the European plan on climate change, which included three “20% targets” [2]. Goals till year 2020 were to reach 20% of renewable energy sources share in Europe, to increase energy efficiency in order to save 20% of energy consumption and to reduce the greenhouse gas emissions by 20%. In order to secure those objectives, several policies were introduced in the European countries. For example Feed-in-Tariff (FiT), as one of the introduced mechanisms, makes sure that renewable energy producer sells electricity on the market at the predefined price for a specific duration of time under specific conditions.

All 27 countries in EU signed a binding contract and have to honour “20% targets” till year 2020. Looking at the Figure 1.1 from 2010, the progress of renewable sources generation from each member state can be analysed. For example Austria had already in 2005 huge amount of renewable energy, but will increase its percentage of renewable sources to 34% by 2020, which would make it the fourth biggest country in Europe by renewable energy share. In Europe, in year 2009, 27.5 GW of new electricity generation was built. Big part, even 62% (17 GW) of newly instalments, was renewable. If the growth continues in expected manner, 35-40% of electricity generation will come from renewable energy sources in year 2020. Big amount of new installed renewable DEG opens up a lot of new challenges for power grid. This is why, 21st century is also called smart grid era [3]. The term smart grids refers to a modernization of the power system, so it monitors, protects and optimizes operation of its interconnected elements.

One among many problematic areas that needs attention is protection system for islanding detection and prevention. Analysis of anti-islanding protection methods in inverter

1 Introduction



Figure 1.1: Mandatory national targets for all EU member states, adopted from [2]

connected Distributed Energy Resources (DER) will be thematic of this master thesis.

1.1 Islanding operation - definition

Definition of islanding operation, adopted from [4]:

“A portion of utility system that contains both load and distributed resources remains energized while it is isolated from the remainder of the utility system.”

Such an undesired event could happen due to circuit tripping, accidental disconnection of the utility through equipment failure, human error, disconnection for maintenance services or network reconfiguration.

For easier understanding of the islanding operation definition, Figure 1.2 should be looked at. Photovoltaics (PV) Array is with inverter at the Point of Common Coupling (PCC)

1.1 Islanding operation - definition

connected to the grid through transformer and utility breaker. RLC-Load is also connected at the PCC. For the actual formation of the islanding, the power from the grid to the load $\Delta P + j\Delta Q$ has to be insignificant at the time right before breaker opening. In that case, generation of the PV array practically covers the consumption of RLC-load and the classical voltage and frequency relays in inverter are not able to detect the islanding [5].

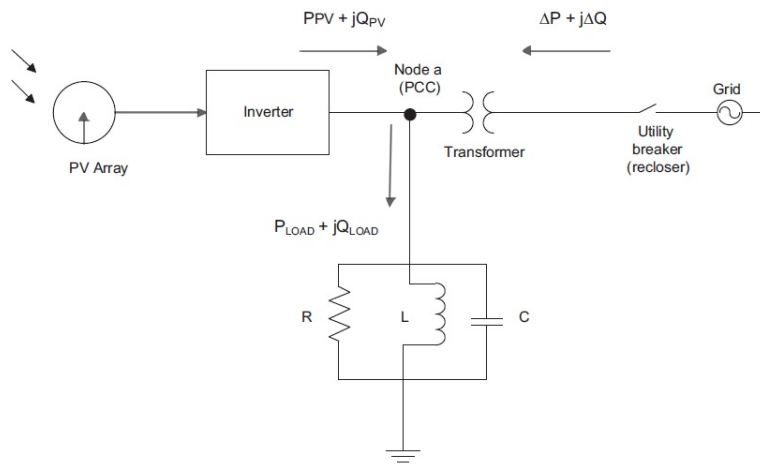


Figure 1.2: Basic configuration for presentation of islanding, adopted from [4]

1 Introduction

Islanding can have following unwanted consequences:

- Danger for the utility personnel, who may intervene on parts of network which should be isolated, but are still energized by the Distributed Generation (DG).
- Adverse impact on the equipment and customers within the islanded area.
- Damage of electrical equipment by out-of-phase closure when, after a fault, the unwanted island is reconnected to the network by automatic reclosing of utility breaker.

In order to avoid these consequences, the protection should prevent islanding as fast as possible. According to [4], different methods for preventing the islanding exist. They are divided into passive, active and remote islanding techniques. In this thesis, passive protection techniques will be precisely analysed.

1.2 Structure of the thesis

In Chapter 2, the master thesis from Dipl.-Ing. David Springer [6] will be shortly summarized, because it will serve as a starting point for further work on current thesis. First, the main conclusions from thesis's theoretical research will be presented, since the research was done for many available anti-islanding protection methods. The main results gathered from implementation of over/under voltage and frequency protection methods in MATLAB/SIMULINK model will also be presented.

Chapter 3 will offer theoretical background for current thesis. Starting with explanation of the islanding problem in bigger sense, in connection with dispersed generation European problem. Behaviour and requirements of inverter connected generation units on the distribution grid will be presented. Further emphasis will be on detailed explanation of the passive anti-islanding protection methods. Different regulating strategies of inverter will also be looked at.

In the 4th Chapter the preparation of MATLAB/SIMULINK model will be explained and

presented in detail, since the model and its results will serve as a thesis's scientific contribution. Analytical gathered Non Detection Zones (NDZ) for different inverter regulations will also be observed.

Analysis and comments of the results from implemented methods in MATLAB/SIMULINK model will be offered in Chapter 5.

The Chapter 6 will conclude the thesis with crucial findings. The challenges for the future work based on this thesis will also be pointed out.

2 State of the art

Main points from Dipl.-Ing. David Springer's master thesis [6] will be presented in the following chapter. The findings from his thesis will serve as a starting point for further research in the area - Analysis of detection methods for preventing islanding operation.

2.1 Theoretical findings

Theoretical research of regulations of inverters on the distribution network and overview of anti-islanding detection methods were done in [6].

- **Regulation of inverters on the distribution grid:** The behaviour of inverter connected generation units on distribution grid is described and specified in Austrian grid code - "Technische und organisatorische Regeln für Betreiber und Benutzer von Netzen" (TOR). Inverter based DEG unit must be able to split from the distribution network at decoupling point during all times in order to prevent islanding. Two most common methods for anti-islanding are voltage and frequency protection. As an example, Table 2.1 shows protection set points for these two methods. Set-points are gathered from TOR for inverters on low voltage (LV) grids.

If triggering of protection relay separates generation unit from the grid, certain conditions have to be fulfilled before it can be coupled with the grid again. These conditions are:

1. $U \geq 0.85 * U_N$ and $U \leq 1.09 * U_N$
2. $47.5 \text{ Hz} \leq f \leq 50.05 \text{ Hz}$
3. 5 minutes delay time before re-coupling is recommended, when both above-mentioned conditions are fulfilled.

Table 2.1: Protection set points for inverters on LV grid, adapted on basis [6]

Function	Set value	Protection delay
Over-voltage protection $>>$	$1.15 * U_N$	≤ 0.1 s
Over-voltage protection $>$	$1.11 * U_N$	≤ 0.1 s
Under-voltage protection $<$	$0.8 * U_N$	≤ 0.2 s
Over-frequency protection $>$	51.5 Hz	≤ 0.1 s
Under-frequency protection $<$	47.5 Hz	≤ 0.1 s
Network failure		≤ 5 s

If required, inverter connected DEG units have to offer certain reactive power support for the grid in order to ensure voltage stability. Following reactive power regulation strategies can be demanded from grid operator:

- power factor $\cos\varphi$
- power factor/active power $\cos\varphi(P)$
- power factor/voltage $\cos\varphi(U)$
- reactive power/voltage $Q(U)$
- specified reactive power output Q

In Figure 2.1, the example of statics for $\cos\varphi(P)$ regulation strategy can be seen. Generation unit must ensure operation with $\cos\varphi = 0.9$ under excited, when active power output is maximum. This method however does not have any influence on voltage stability in the area $0 \leq P \leq 0.5 * P_N$.

In addition to reactive power support, active power support to the grid can also be required from system operator. Active power regulation strategy could for example be given with active power/frequency statics $P(f)$.

- **Anti-islanding detection methods:** One of the most important criterion for description of anti-islanding protection method is Non-Detection Zone: NDZ is an area, where protection method cannot detect the islanding and protection does not trigger. NDZ can be determined for the majority of active and passive techniques and is consequently a good criterion for sorting the effectiveness of individual methods.

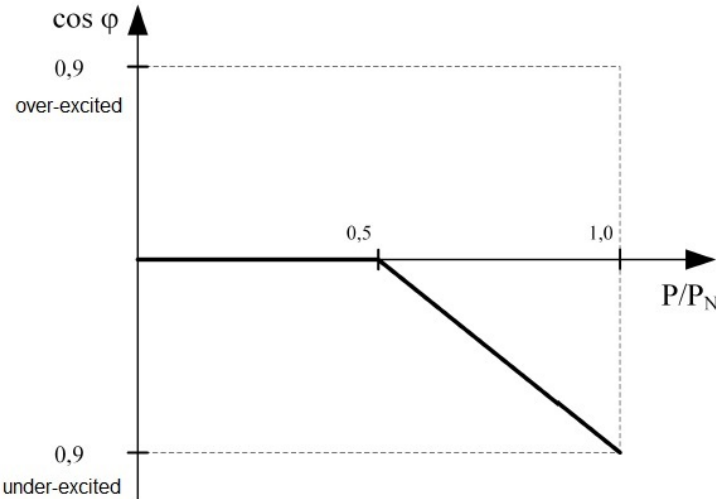


Figure 2.1: Statics for $\cos\varphi(P)$, adapted on basis [6]

An example of NDZ for voltage and frequency protection methods can be seen in Figure 2.2.

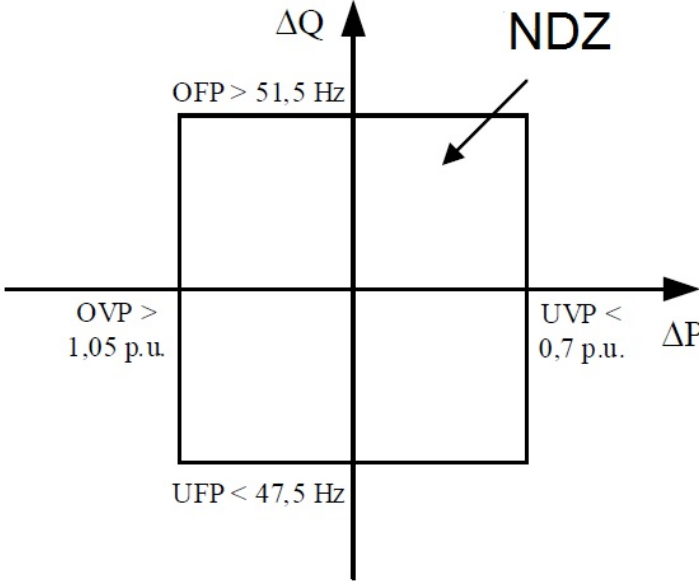


Figure 2.2: NDZ, adapted on basis [6]

Table 2.2 gathers the knowledge on different anti-islanding protection methods and gives the overview of advantages and disadvantages of the researched techniques.

2 State of the art

Table 2.2: Overview of advantages and disadvantages of anti-islanding protection methods, adapted on basis [6]

Passive/Active	Category	Detection Method	Influencing detection sensitivity with multiple inverters	Influencing voltage quality and stability	Reaction time	NDZ	Determination of limit values	Costs
Passive	Voltage	Voltage and frequency monitoring	No	No	Long	Big	Easy	Low
		Harmonic distortion monitoring	Yes	No	Medium	Small	Difficult	Low
		Rate of change of frequency	Yes	No	Medium	Small	Difficult	Low
	Voltage and Current	Phase-jump	Yes	No	Short	Small	Difficult	Low
		Rate of change of active power	Yes	No	Medium	Small	Difficult	Low
	Communication	Power line carrier communication	No	No	Short	No NDZ	Not needed	High
Signal produced by disconnect		No	No	Short	No NDZ	Not needed	High	
Active	Intervention on DEG	Impedance measurement	Yes	Yes	Medium	Small	Moderate	Low
		Frequency modulation	No	Yes	Short	Very small	Not needed	Low
		Phase modulation	No	Slight	Short	Very small	Not needed	Low
	Intervention on Network	Impedance On/Off	No	No	Medium	Very small	Not needed	High
		Phase modulation	No	No	Short	Very small	Not needed	Low

2.2 Thesis's conclusion

Over/under voltage protection (OVP/UVP) methods and over/under frequency protection (OFP/UFP) methods were implemented in MATLAB/SIMULINK model. For evaluation of these methods, detection times and NDZs of the methods were acquired. Three different regulating strategies of inverter were simulated in the case study in order to show how the area of NDZ changes:

1. Only active power output
2. Active and reactive power output with constant $\cos\varphi$
3. Active and reactive power output with constant $\cos\varphi$ and active power reduction by over-frequency

NDZs in cases of three different regulating strategies of inverter are presented in Figure 2.3. Black lines in the figures present analytically calculated NDZ areas - for comparison to simulated NDZ areas. Furthermore, the punctured area in Figure 2.3 below shows the area of NDZ change, when active power reduction by over-frequency is introduced. The NDZ gets slightly bigger, because active power reduction at high frequencies acts towards stabilizing of the island. Therefore, islanding detection is more difficult.

2.3 Further work

This thesis will continue work done in master thesis [6]. The scientific contribution of the work will be based on observation of further regulating strategies of inverter. More specifically, NDZ will be observed as a function of:

- reactive power/voltage $Q(U)$
- power factor/active power $\cos\varphi(U)$
- active power/voltage $P(U)$

Furthermore, the behaviour of frequency and voltage during the transition period from the state of grid connected mode to the state of island mode, for cases when OVP/UVP and OFP/UFP threshold values are not exceeded, will be carefully looked at. The goal of this

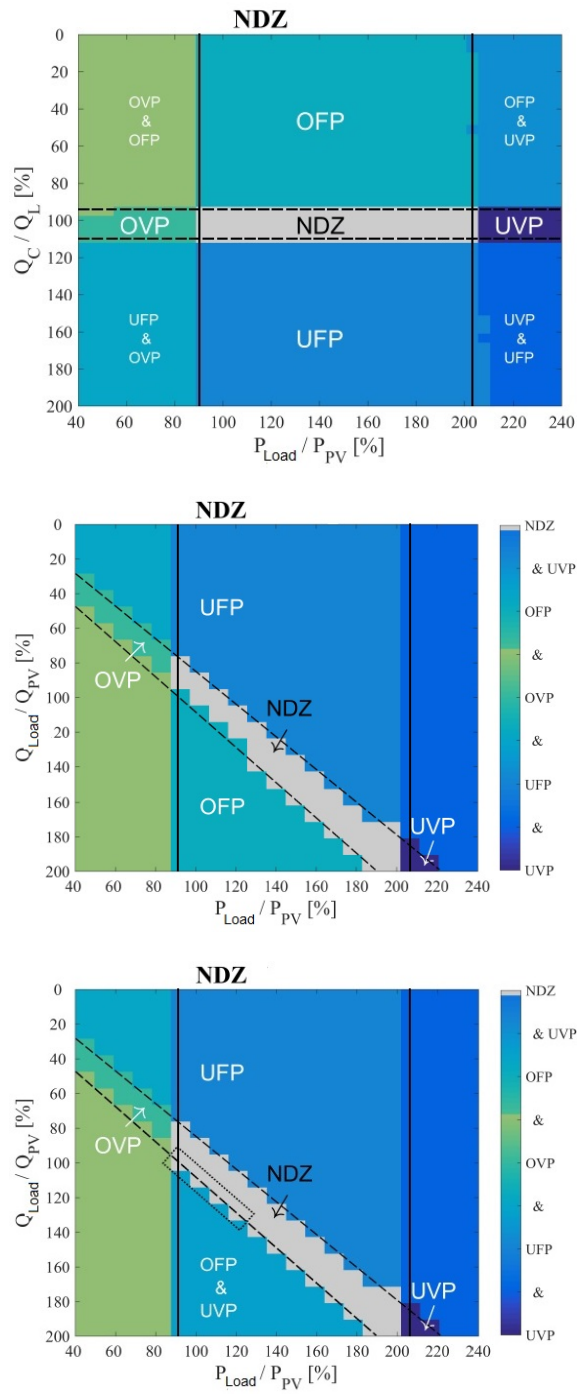


Figure 2.3: NDZ: Only active power output (above), Active and reactive power output with constant $\cos\phi$ (middle), Active and reactive power output with constant $\cos\phi$ and active power reduction by over-frequency (below), adopted from [6]

2.3 Further work

observation will be to critically assess, if the possible dynamic behaviour during transition would be potentially appropriate for introduction of additional protection methods for prevention of unwanted islanding.

3 Theoretical background

3.1 Dispersed generation problem in context with islanding

Islanding or loss-of-mains is part of the bigger problem, concerning the power grid of the continental Europe. According to the report [7] from year 2013, written from European Network of Transmission System Operators for Electricity (ENTSO-E), there were approximately 52 GW of installed power capacity coming from PV and approximately 62 GW from wind and other distributed generation in continental Europe. Knowing that load of the whole continental Europe is between 220 GW and 440 GW, dispersed generation presents a massive share for covering electricity consumption. European electricity system operates in synchronous way, frequency is identical everywhere. Deviation of the frequency from 50 Hz results in activation of one of the regulating controls (primary, secondary...), based on the severity of the violation deviation. At the time of the report (year 2013), most of the dispersed units had frequency protection settings that were not compliant with frequency setting of the transmission system. Thresholds for dispersed generation disconnection were between 50.2 Hz - 50.3 Hz for over-frequency and 49.7 Hz - 49.5 Hz for under-frequency, although range of frequency for transmission system is between 47.5 Hz - 51.5 Hz. Frequency deviations during events like loss of 2 GW load or 3 GW generation led to uncoordinated disconnection of distributed generation and consequentially to load shedding in order to secure the stability of the system. Report [7] worked on dynamic model of continental Europe's analysis and among other things researched appropriate disconnection settings for dispersed generation.

According to [8], the first standard for prevention of islanding arised in 1999 in Germany, because of the huge growth of PV units on the grid. This standard, DIN VDE 0126-1-1 prescripts operation and testing of protection device, which prevents islanding. The standard was/is beside Germany also used in Austria, Belgium, France and Switzerland.

3 Theoretical background

Protection devices should, according to standard, measure frequency, voltage and grid impedance. In cases, when those measurements are outside the pre-scripted band, the device should disconnect the inverter from the grid. DIN VDE 0126-1-1 was renewed in 2005 and then again in 2013, because additional growth of generation units and new challenges on the grid required adjustments, especially in terms of protection limit values. Threshold values and other requirements are furthermore determined from grid operator in compliance to a specific situation of each new generation unit connected on the grid. In Austria, new requirements for generation units on the distribution grid were introduced with TOR D2 in year 2016 (old version is from 2013), [9]. Inverter connected DER's requirements are also part of this segment of TOR and are therefore interesting for this thesis. Some requirements were already described in Chapter 2, as part of Springer's master thesis [6]. Further features will be explained in next section.

3.2 Requirements for connection of inverter connected DER on the grid

TOR D2 [9] features technical and organisational rules for all electricity generation units, that are connected in medium or low voltage grid (Parallelbetrieb von Erzeugungsanlagen mit Verteilnetzen). Inverter connected generation units on medium voltage (MV) grid (simulation model in Chapter 4 is made on medium voltage grid) are interesting for the purposes of this thesis and requirements for those will mostly be looked at in the following subsections.

Generation units on the distribution grid must be provided with switching and decoupling point.

- **Switching point** has to be accessible by grid operator for reasons of operational management and personal safety. It should have disconnecting function and load switching capacity. It should also be compliant with five safety regulations according to standard ÖVE EN 50110-1.
- **Decoupling point** has to be used to connect generation unit to the mains. This point ensures all-pole galvanic separation of the generating system from the mains.

3.2.1 Behaviour of inverter connected generation units on distribution grid

Inverter connected generation units on medium voltage grid should ensure certain static and dynamic support for the mains. Three possible reactive power areas can be demanded from the grid operator for generation units with apparent power $S_r > 3.68$ kV A. Those areas are presented in Table 3.1.

Table 3.1: Reactive power areas for medium voltage grid, adopted from [9]

	Demand	$\frac{Q_{max}}{S_r}$	$cos\varphi$ at Q_{max} and S_r
Connection in medium voltage grid at $P \geq 20\% S_r$	I	-43.6% to 31.2%	0.90 under-excited to 0.95 over-excited
	II	$\pm 38\%$	0.925 (under-excited/over-excited)
	III	-31.2% to 43.6%	0.95 under-excited to 0.90 over-excited

Demand II from the Table 3.1 is most commonly required for connection to MV grid and it was also chosen for simulations in this thesis (more in Chapter 4). Demands I and III are required only in specific and justified situations. Reactive power areas from the previous table are easier presentable in Figure 3.1.

3.2.2 Inverter regulation strategies

Most common inverter regulation strategy is only active power injection into the grid, $cos\varphi = 1$. Based on positioning of the generation unit on the grid, grid load and injected power, one of the following reactive power support possibilities can be required from inverter connected generation unit:

- power factor, $cos\varphi$
- power factor/active power, $cos\varphi(P)$
- power factor/voltage, $cos\varphi(U)$
- reactive power/voltage, $Q(U)$

3 Theoretical background

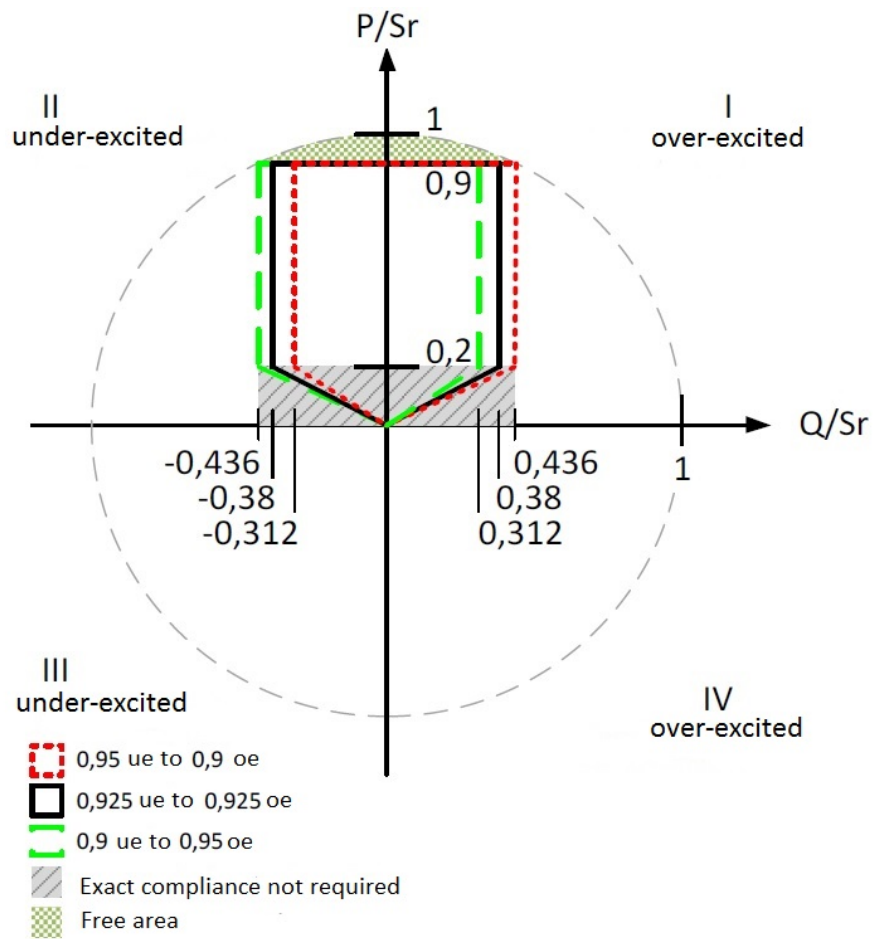


Figure 3.1: Reactive power areas, adapted on basis [9]

3.2 Requirements for connection of inverter connected DER on the grid

- specified reactive power output, Q

Active power support possibilities:

- active power/frequency, $P(f)$ ¹
- active power/voltage, $P(U)$
- specified active power output, P

If the apparent power of the unit is more than 100 kV A, then reactive power set points could be given online, in the real time.

In the scope of the thesis, NDZ will be observed as a function of $Q(U)$, $\cos\varphi(U)$ and $P(U)$ inverter regulations and therefore only these three regulation strategies will be presented further into detail.

$Q(U)$ inverter regulation

Figure 3.2 shows example of $Q(U)$ inverter regulation statics for LV grids. Four control points (a, b, c, d) of the statics can be parametrized for desired regulation. In the area between points b and c, the DER has output power with $\cos\varphi = 1$, so only active power output. If the voltage gets above point c or beyond point b, the inverter of DER has to output power with fitting reactive power, which can be specified from the statics. The maximum required value of reactive power $\frac{Q}{S_r}$ is 43.6% over/under excited for LV grids. This value corresponds with points a and d in the Figure 3.2. $Q(U)$ inverter regulation should be applied to each voltage phase. If it is not applied to each phase, then all three phases are regulated symmetrically on the basis of the highest voltage in one of the phases.

$\cos\varphi(U)$ inverter regulation

Even though TOR D2 does not feature this requirement for DER (it is only possible for special arrangements), inverter regulation $\cos\varphi(U)$ will be investigated in the thesis. In-

¹As an answer to the problem from report from ENTSO-E (disconnection of generation units at over-frequency of 50.2 Hz), [7] - following regulation is proposed: Reducing of active power output for 40% of current active power (P) per each Hertz in the area from 50.2 Hz to 51.5 Hz.

3 Theoretical background

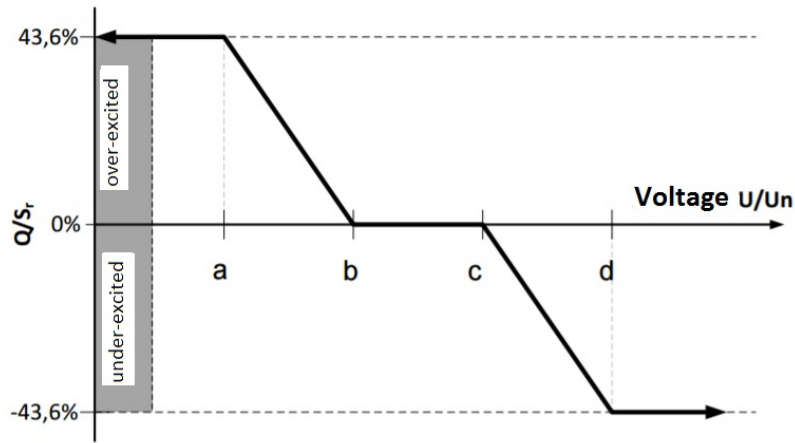


Figure 3.2: Q(U) curve for LV grids, adopted from [9]

verters have the possibility to execute $\cos\varphi(U)$ regulation and therefore the observation of its impact on NDZ is meaningful. Figure 3.3 shows an example of the proposed regulation curve. It was gathered from parametrization of PV inverters, summarized by one of the grid operators in Austria, Salzburg Netz GmbH, [10]. It can be concluded from the figure, that parametrization was done point by point, for desired values of voltage. Since rules for this regulation are not specified in TOR D2, the $\cos\varphi(U)$ curve for this thesis will have to be obtained with heuristic approach.

$P(U)$ inverter regulation

Two types of $P(U)$ regulations are possible. One possibility is to reduce maximal possible active power of the generation unit at specified voltage set point. The other possibility is to reduce current active power (active power at the time, when voltage set point is exceeded). First possibility is presented in Figure 3.4, reducing maximal possible active power of the unit. The same inverter regulation is also used in the simulation model (more in Chapter 4). Active power output of the DER is regulated based on the voltage. When voltage is higher than U_{knick} , the output power of DER is reduced from $100\% P_n$ to $0\% P_n$ in the linear manner. Selection of $U_{knick} = 110\% U_n$ ensures, that generation unit does not operate in unwanted over- voltage area.

3.2 Requirements for connection of inverter connected DER on the grid

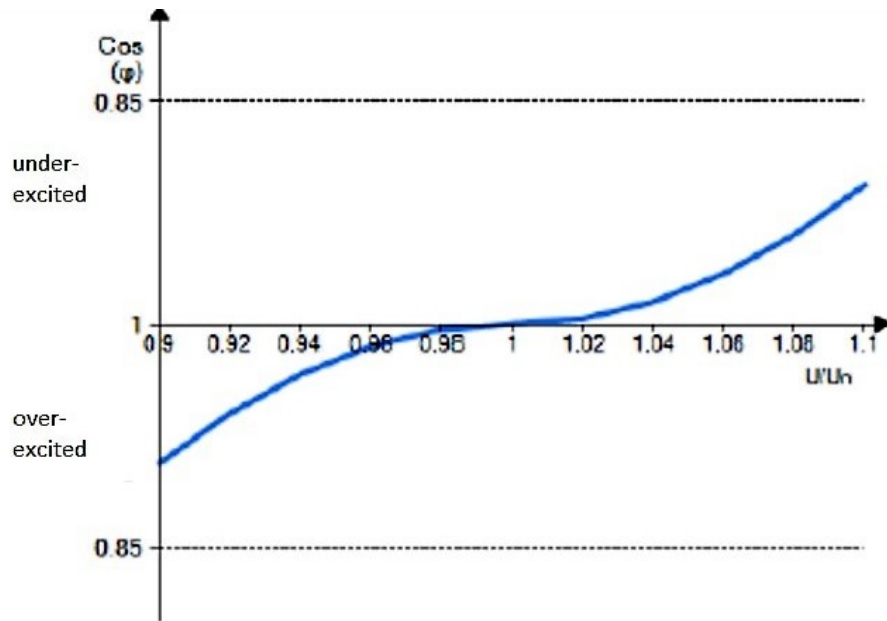


Figure 3.3: $\cos\varphi(U)$ curve, adopted from [10]

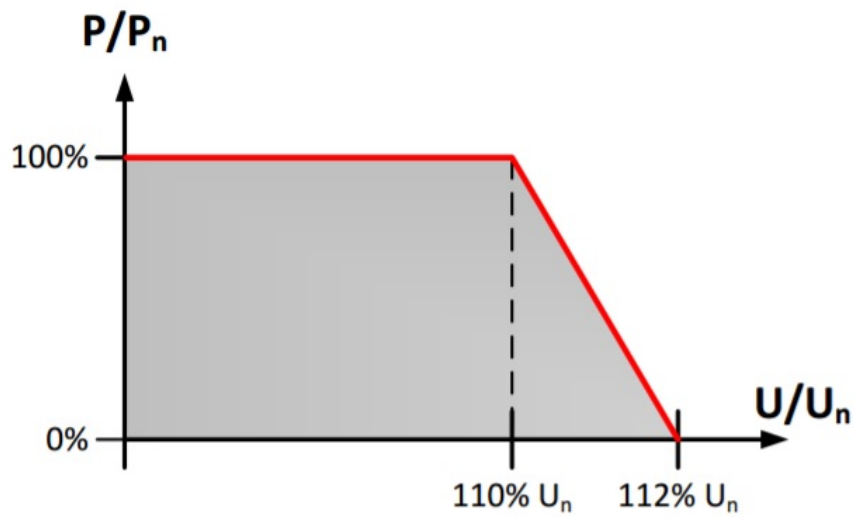


Figure 3.4: $P(U)$ curve, adopted from [9]

3.2.3 Protection for decoupling point

Protection for the decoupling point has the task to disconnect the generation unit, if problematic operating conditions arise. Inverter takes over the role of protection for decoupling point, if generation unit is inverter connected to the grid. Following protection functions can be applicable for decoupling point:

- Voltage protection function
- Frequency protection function
- Ground fault protection
- Reactive power - under voltage protection (Q_{-} & $U <$)
- Others

3.3 Protection methods

Protection methods for anti-islanding are divided in active, passive and remote methods.

- **Passive methods** work based on measuring system parameters, such as voltage, frequency and harmonic distortion. If islanding occurs and protection threshold values for these parameters are properly established, deviations from normal values (operation in grid mode) could usually be detected and the protection is able to trigger. Setting of the appropriate threshold values is one of the biggest challenges. Passive detection techniques are usually fast, but have rather big NDZ. Costs connected with this type of methods are commonly on the low side, because some of the methods are already implemented in inverter-relays for basic protection functions. Multiple inverters in the island area usually do not cause detection problem in the case of passive protection techniques.
- **Active methods** inject disturbances in the inverter outputs (for example: small perturbation in output current waveform). Influences of disturbances are negligible in grid mode, but can be effectively detected when utility breaker is open. The setting of threshold values for perturbations are again big challenge. Inappropriate threshold settings can cause tripping of DERs in grid mode. If values are properly

adjusted, the NDZ can be very small and active methods can be very effective and quick.

- **Remote methods** use communication between utility and DER for islanding detection. Transmitter on the utility side of the grid is sending the signal, receiver on the DER side of the grid is receiving the signal. When the utility breaker is opened, the signal is sent to receiver and as a result DERs disconnect from the grid. Remote techniques are very reliable, but are also connected with huge costs for transmitter and receiver devices. Investment in this additional equipment could make the installation of DER uneconomical.

Active and remote protection methods will not be analysed further in the scope of this work, therefore only individual passive protection techniques will be thoroughly described in the following. Different literature sources were used for this section: [4], [11], [12], [13].

3.4 Passive Methods

3.4.1 Over/under voltage and over/under frequency protection method

Implementation of OVP/UVP and OFP/UFP methods is required in all inverter-connected DERs. This protection is primarily installed for the protection of loads and customers' equipment, but can also serve as a protection against islanding. Based on Figure 3.5, equations 3.1 and 3.2 can be carried out and analysed. $\Delta P + j\Delta Q$ is the power from the grid, $P_{PV} + jQ_{PV}$ is power from the DER (in this case PV) and $P_{load} + jQ_{load}$ is power flow to the load. When $\Delta P = 0$, $\Delta Q = 0$ and the utility breaker opens, the following conclusions can be made: there is an active and reactive power match between DER and load. OVP/UVP, OFP/UFP protections will not detect any voltage and frequency changes, therefore the protection relay will not trigger. However, when $\Delta P \neq 0$ and $\Delta Q \neq 0$ (active and reactive power mismatch), which is the case most of the time, then voltage and frequency deviations will be the reason for protection devices triggering, if the deviations are above the threshold values.

$$\Delta P = P_{load} - P_{PV} \quad (3.1)$$

$$\Delta Q = Q_{load} - Q_{PV} \quad (3.2)$$

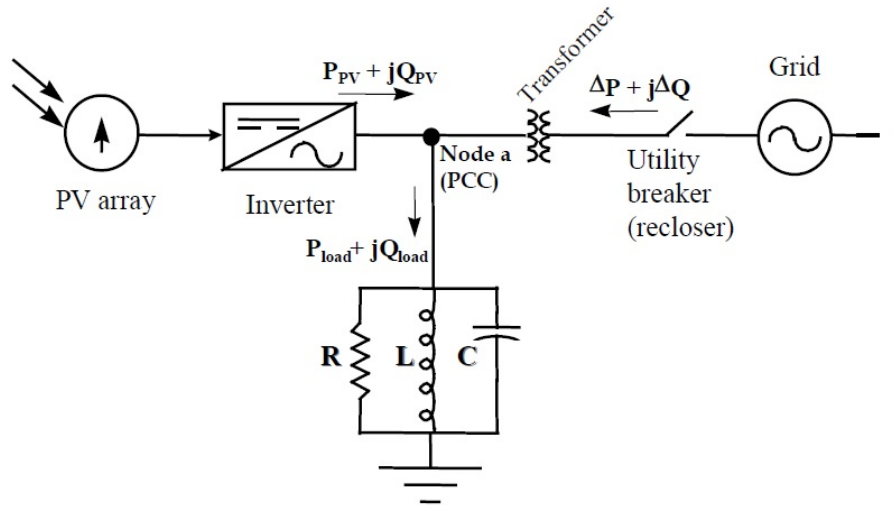


Figure 3.5: Feeder configuration showing power flows, adopted from [11]

Strengths and weaknesses

OVP/UVP and OFP/UFP methods are connected with low costs, because these methods are already implemented in inverter connected DERs. The biggest weakness is relative big NDZ. Threshold values are determined in TOR and were for example of LV grid already presented in Table 2.1, in Chapter 2. If lower limit values would be defined, the NDZ would also be smaller, but it could lead to protection triggering in grid mode.

3.4.2 Phase jump detection method

Phase jump protection method monitors phase difference between voltage and current output of DER. In the case of current-source inverters, inverter's output current is synchronized with utility voltage at PCC (Figure 3.5) every time, when rising or falling zero crossing of voltage at PCC is detected. Synchronization is done by phase-locked-loop (PLL) - control system that generates an output signal, whose phase is related to the input signal. In case of voltage-source inverter the roles of voltage and current are exchanged.

When island is formed, the phase angle of the load should be the same as it was before

the island was formed. As can be seen in Figure 3.6, the output current of DER stays the same even after islanding, because it is fixed with PLL. The output voltage of DER is however not fixed with utility voltage anymore and in order to maintain the same phase angle of the load before islanding, voltage has to “jump” to the new phase. If the phase error between current and voltage is above threshold value it can be detected at the next zero crossing.

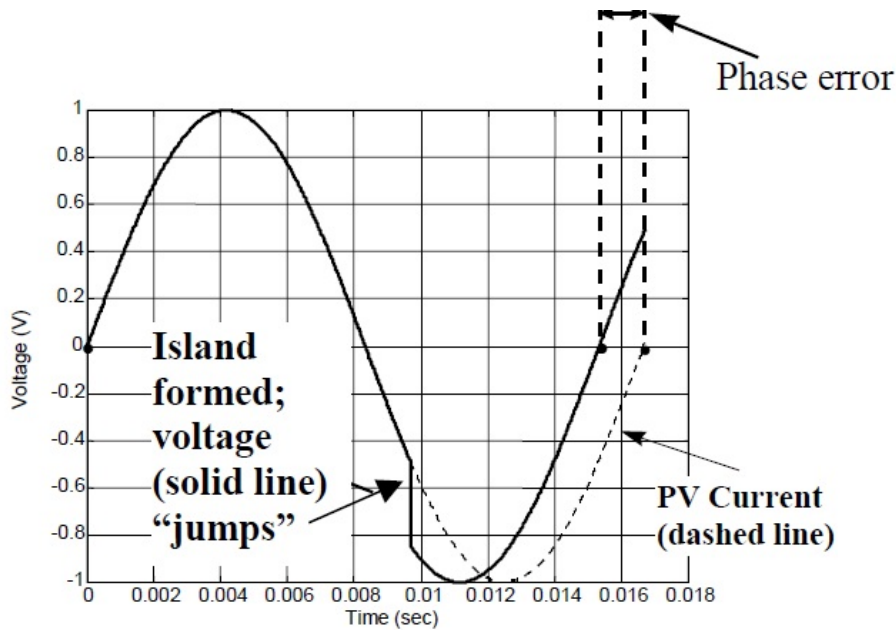


Figure 3.6: Operation of the phase jump detection method, adopted from [11]

Strengths and weaknesses

Strength of the method is the ease of implementation, since PLL is needed in inverter for utility synchronization anyway. Weakness of the phase jump detection method is setting the correct threshold value, with which reliable detection of the islanding operation is possible.

3.4.3 Detection of harmonics

This method monitors the voltage and its Total Harmonic Distortion (THD) at PCC (Figure 3.5). The protection triggers if the THD exceeds specified threshold. When utility breaker is closed, the voltage at PCC is determined with “rigid” grid and almost

3 Theoretical background

none THD is expected. Output current of the DER always has some amount of THD, but when it flows to the low impedance utility grid, it produces only small amount of voltage distortion at PCC. When island is formed, the impedance of load is higher in comparison to the grid. Output current of DER in interaction with “island load” produces bigger distortions of voltage at PCC and islanding can be detected.

Strengths and weaknesses

Detection of harmonics protection method can be very effective under certain conditions (for example: if threshold value is successfully set). There is normally huge difficulty in finding an appropriate limit value of THD. Selected threshold THD value must be higher than distortions values in grid mode and lower than distortions values in island mode.

3.4.4 Rate of change of frequency (ROCOF)

Voltage waveform is observed in the rate of change of frequency (ROCOF) protection method . When $\frac{df}{dt} >$ threshold value, inverter shuts down. This usually happens when island is formed and there is a mismatch between DER production and load consumption. In the transient period, between grid mode and island mode, the frequency changes, if there is power imbalance. According to [12], ROCOF can be described with equation 3.3.

$$ROCOF = \frac{df}{dt} = \frac{\Delta P}{2 * H * G} * f \quad (3.3)$$

ΔP is power mismatch on DER’s side, H is moment of inertia and G is rated generation capacity of DER.

Strengths and weaknesses

ROCOF protection method is effective and reacts faster than OFP/UFP. It is especially effective in cases of big power imbalance. The challenge is to find the right trip setting value in order to prevent shutting down inverters in grid mode.

Research of ROCOF threshold settings values

Frequency deviations or jumps are caused by power imbalances between generation and load. Power imbalance is compensated with change of kinetic energy of generators and motors and therefore frequency stabilizes. According to [14], most frequency deviations occur at quarterly, half-hourly and hourly transitions, because of economic dispatch of generating power plants or in other words - because of electricity markets. Especially problematic are morning and evening peak hours, when consumption is changing rapidly. Producers, consumers and electricity traders are in the markets represented by Balance Responsible Parties (BRP). The goal of BRP is to maximize their profits, with adjusting the selling of electricity at the right time. BRPs are constrained with energy exchange in Program Time Unit (PTU). Figure 3.7 offers further explanation of the latter. As can be seen in the figure, BRP does not need to match the load in the real time, it only needs to exchange the agreed amount of power in the PTU. PTU lengths differ from country to country. For example in Austria, the duration of PTU is 15 minutes, as is the case in Germany, Italy, Netherlands and other countries. It can be concluded from the Figure 3.7, that shorter the duration of PTU, better mitigation to frequency deviations can be offered.

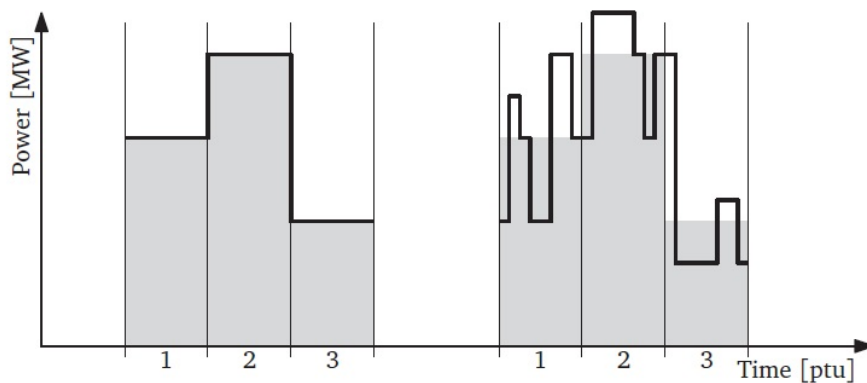


Figure 3.7: A BRP is only constrained by the energy exchange per PTU, adopted from [14]

Source [14] also provided recording of the frequency for the period from March 2008 to February 2009. Monthly and yearly averages were calculated and presented for the whole

3 Theoretical background

day. Figure 3.8 presents only part of the day, namely evening hours, where frequency deviations were the biggest. The biggest frequency leaps were recorded at hourly trading.

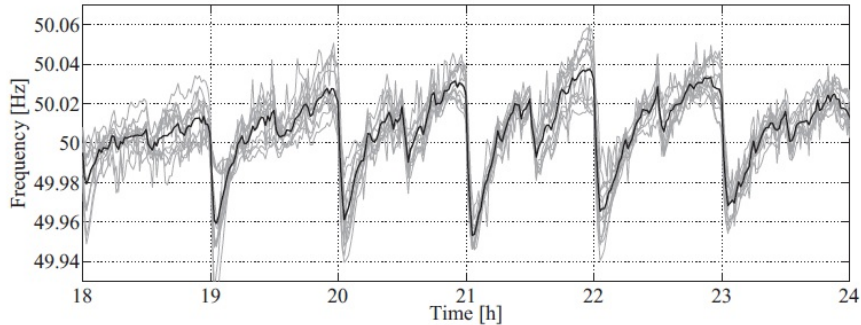


Figure 3.8: Monthly and yearly averages of frequency deviations in the period from March 2008 to February 2009, adopted from [14]

Exact numbers for ROCOF were for example found in report from year 2013 from Commission for Energy Regulations (CER), [15]. This report focused on the problematic for ROCOF threshold values in Ireland. Report dealt with the problematics of raising the maximum value of 0.5 Hz s^{-1} to 1 Hz s^{-1} , measured over 500 ms period. This value is compatible with proposed standard in Great Britain, where values are between 1 Hz/s and 2 Hz/s . Values for ROCOF in one of the newest papers [16] are also set at 2 Hz s^{-1} . In conclusion it could be said, that threshold values for df/dt are subject of evaluation and therefore frequency jumps in simulations of this thesis (Chapter 5) will be evaluated in order to propose the possible appropriate limit.

3.4.5 Other passive methods

Rate of change of output power (ROCOP) is also one of the possible protection methods for anti-islanding. It works on similar basis as ROCOF. Namely, when $\frac{dP}{dt} >$ threshold value, protection triggers. The change of output power of DER is much higher for load change in case of island mode operation than in case of grid mode operation and therefore islanding operation can be detected.

Another possibility is to observe **Rate of change of frequency over power (RO-**

COFOP). According to [12], the change of frequency over power is much bigger than change of frequency over time for small power mismatch between DER and load.

Comparison of rate of change of frequency (COROCOF) compares the change of frequency at two locations: on the grid side and at the DER. The practical implementation of the method is however difficult, due to much computational work.

4 Analytical background

4.1 MATLAB Simulink model

4.1.1 Basic description

Simulation model for the purposes of this master thesis was made in MATLAB Simulink. Model was created on the basis of “Detailed Model of a 100-kW Grid-Connected PV Array”, which is one of the accessible models in Simulink for Simscape Power Systems. Changes were made to the basis model in order to simplify individual features and to adjust them for the purposes of anti-islanding detection. The following chapter will introduce model’s main features, while also explaining additions and changes. Schematics of the model and its essential elements can be seen in the Figure 4.1.

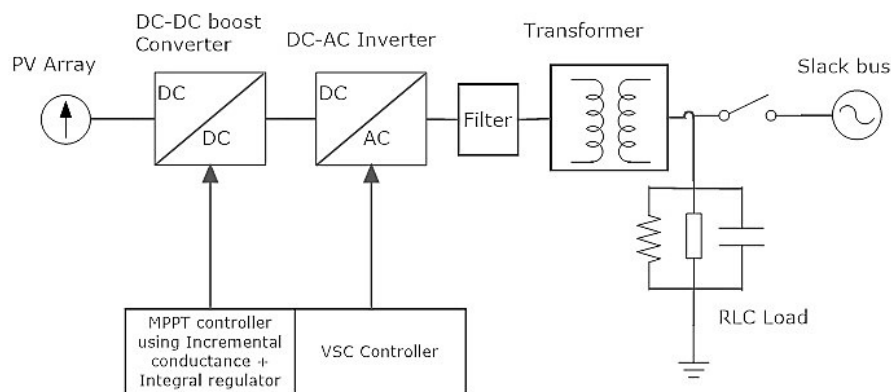


Figure 4.1: Schematic representation of Simulink model, made with SmartDraw2017

- **PV Array:** PV Array consists of 66 strings of 5 series-connected modules connected in parallel, [17]. Original output power of array was 100.7 kW, but was increased for factor 10 (more specifically, number of strings was increased for factor 10) in order

4 Analytical background

to get approximately 1 MW of power injection into the grid. All corresponding loads and filters in the model were also adjusted with the factor 10 in order to ensure unchanged circumstances for power injected into the grid. The actual active power injected into the grid after changes was approximately 975 kW. PV Array's output in the original Simulink model can be influenced by irradiation and temperature, as is the case in the natural circumstances. Irradiation and temperature changes are however not the primary focus, when anti-islanding protection is in question. Therefore, the constant irradiation of 1000 W m^{-2} and temperature of 25°C (optimal conditions for PV) were set for the duration of simulations.

- **DC-DC boost converter:** DC-DC boost converter increases the voltage from 273V DC (DC voltage at PV at maximum power) to 500 V DC. Maximum Power Point Tracking (MPPT) system is used by this converter to ensure the appropriate voltage for maximum power output of PV array, [18]. Several techniques are introduced in [19] for MPPT function. Incremental Conductance + Integral Regulator is used in this model. Figure 4.2 presents the power curve of PV Array. It is clearly seen in the figure, that solar modules inject maximum power only at certain voltage or current and slope at that point is 0. Based on this fact, Equations 4.1, 4.2 and 4.3 can be derived.

$$\frac{dP}{dV} = 0, \quad \text{at } MPP \quad (4.1)$$

$$\frac{dP}{dV} > 0, \quad \text{left of } MPP \quad (4.2)$$

$$\frac{dP}{dV} < 0, \quad \text{right of } MPP \quad (4.3)$$

These are followed by Equation 4.4. The MPP is therefore tracked by comparing incremental conductance to instantaneous conductance. Furthermore, integral regulator is used to drive the error e : $e = \frac{dI}{dV} + \frac{I}{V}$ to zero.

$$\frac{dP}{dV} = \frac{d(I * V)}{dV} = I + V * \frac{dI}{dV} \quad - > \quad \frac{dI}{dV} + \frac{I}{V} = 0 \quad (4.4)$$

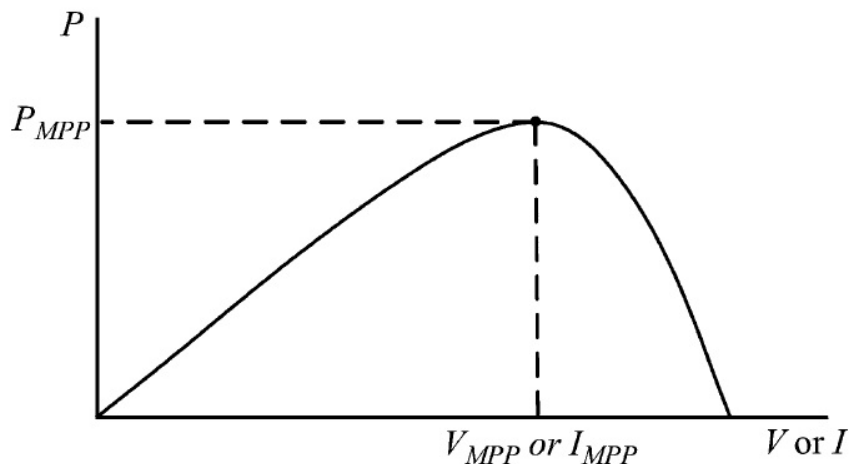


Figure 4.2: Characteristic PV Array power curve, adopted from [19]

- DC-AC Inverter:** DC-AC inverter is used for converting 500 V of DC voltage to 260 V AC voltage, [17]. Inverter is controlled by Voltage Source Controller (VSC), which uses two control loops, [20]. External loop controls DC-Link voltage in order to output the desired active power. Internal loop controls I_d and I_q currents (active and reactive current components). abc-dq transformation is used to transform grid voltages and currents to reference frame voltages and currents. This transformation uses phase angle, which is provided by PLL technique and is needed for synchronizing the controlled current with grid voltage. The reason for abc-dq transformations lies in simplified control of DC values.
- RLC Load:** RLC load was added to the model in order to get the possibility to establish appropriate conditions to observe the protection against islanding.
- Slack bus:** Instead of utility grid from the original model, slack-bus is used for the purposes of this thesis. Slack-bus is the reference bus and offers reference voltage and angle setting, [21]. Furthermore, slack is also used to balance the active and reactive power in the system.

4.1.2 Protection settings

MATLAB Simulink model was further expanded by adding the OVP/UVP and OFP/UFP protection. Model works on a medium voltage network and reference voltage at slack bus is $U_N = 25$ kV, Root Mean Square (RMS), phase-to-phase. Reference frequency is $f_N = 50$ Hz. Threshold values of protection for medium voltage grid can be found in TOR D2, [9]. TOR specifies different limit values for voltage protection: over-voltage protection $>$ and overover-voltage protection $>>$. For example: If voltage is within $1.02 U_N \leq U \leq 1.05 U_N$ for more than 60 seconds, then OVP should trigger. If however voltage is within $1.05 U_N \leq U \leq 1.15 U_N$ for more than just 0.1 of a second, then OVP should also trigger. In order to select meaningful threshold values for the model, combinations acquired with compromise were chosen. Limit values are gathered in Table 4.1.

Table 4.1: Protection set points for inverters on MV grid, adopted from [9]

Protection	Set value	Protection delay
Over-voltage protection $>$	$1.10 * U_N$	≤ 0.1 s
Under-voltage protection $<$	$0.7 * U_N$	≤ 0.1 s
Over-frequency protection $>$	51.5 Hz	≤ 0.1 s
Under-frequency protection $<$	47.5 Hz	≤ 0.1 s
Network failure		≤ 5 s

Figure 4.3 gives an overview of protection functions implemented in MATLAB Simulink model. The addition of “On delay” and “Stop” blocks after each protection function offers the ability to stop the simulation once the protection is triggered. The main reason for latter lies in gaining the time, since the model is slow and there is no use of running it for the whole simulation time, if the protection has already detected the exceeding of threshold values.

4.1.3 Plotting of the NDZ

The main result of the described MATLAB Simulink model is NDZ. NDZ can be plotted in different ways. One possibility is to plot the ratio of active power P_{Load}/P_{PV} on x

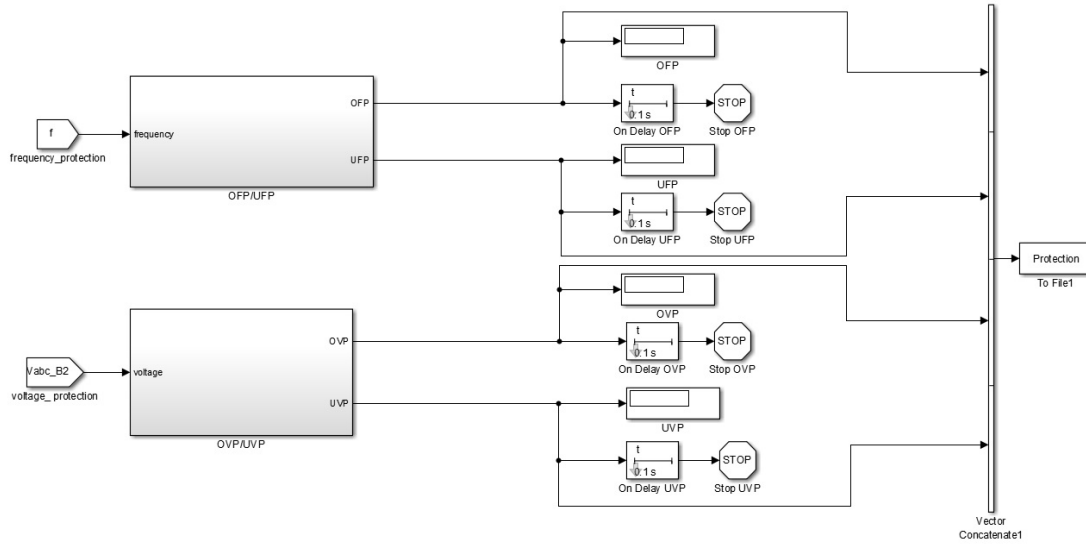


Figure 4.3: OVP/UVP and OFP/UFP protection in MATLAB Simulink model

axes and reactive power Q_{Load}/Q_{PV} on y axes. This kind of presentation was chosen in the Springer's thesis [6], Figure 2.3. It would be meaningful to maintain the same outlook in order to compare NDZs easier, but new presentation of the NDZ was chosen for this thesis due to various reasons. Figure 4.4 shows the example of the chosen depiction. It offers the exact mismatch between load and PV, $\Delta P = P_{Load} - P_{PV}$ on x axes and $\Delta Q = Q_{Load} - Q_{PV}$ on y axes. With this display, it is easier to analyse how far from the exact match or null point certain point of NDZ is. The same display is also used in many papers, for example [22], [23] and [24]. Figure 4.5 shows, how the data for NDZ is gathered in MATLAB Simulink model. Positive sequence of power is calculated from voltages and currents at photovoltaic and load. This data is acquired in "Vector Concatenate" and used for plotting within MATLAB script.

4.1.4 Inverter regulation setting

Further extension of the model was done for different inverter regulations as showed in Figure 4.6. Each of the regulations, namely $P(U)$, $Q(U)$ and $\cos\varphi(U)$ were implemented within MATLAB function and integrated into Simulink. Additional regulation with $P(U)$ and constant $\cos\varphi_{PV}$ was added in order to make a comparison with $P(U)$ regulation.

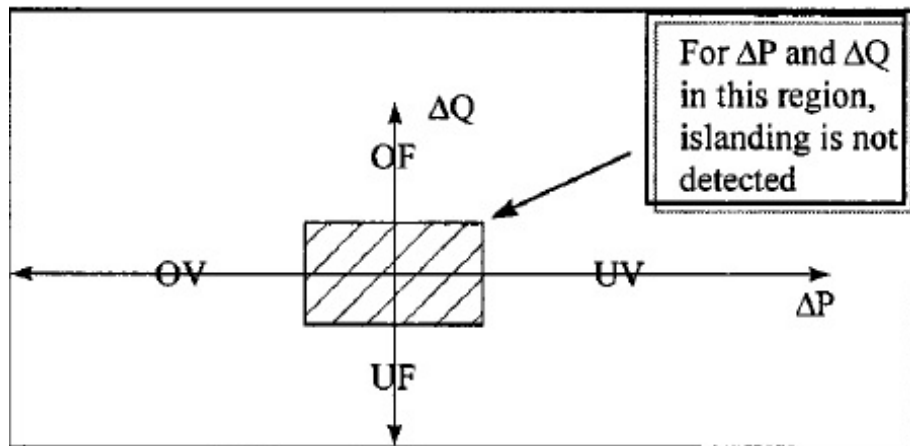


Figure 4.4: Plotting of NDZ, adopted from [22]

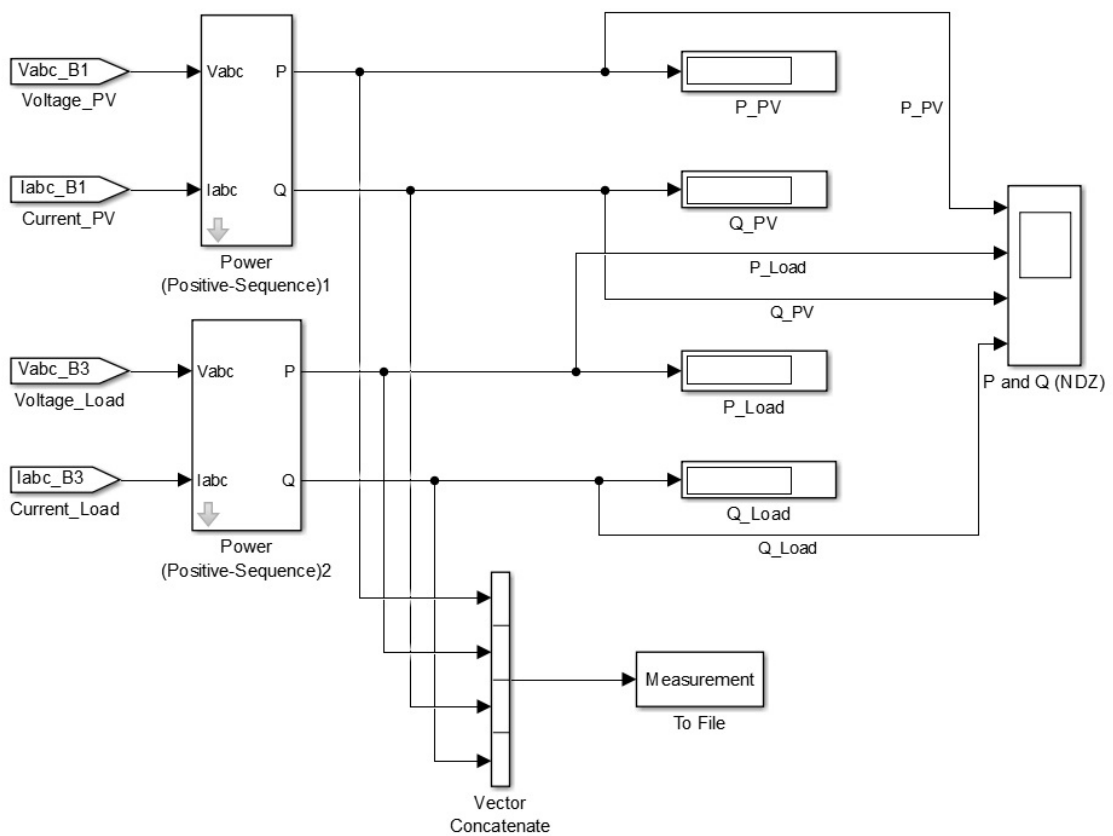


Figure 4.5: Gathering of NDZ in MATLAB Simulink model

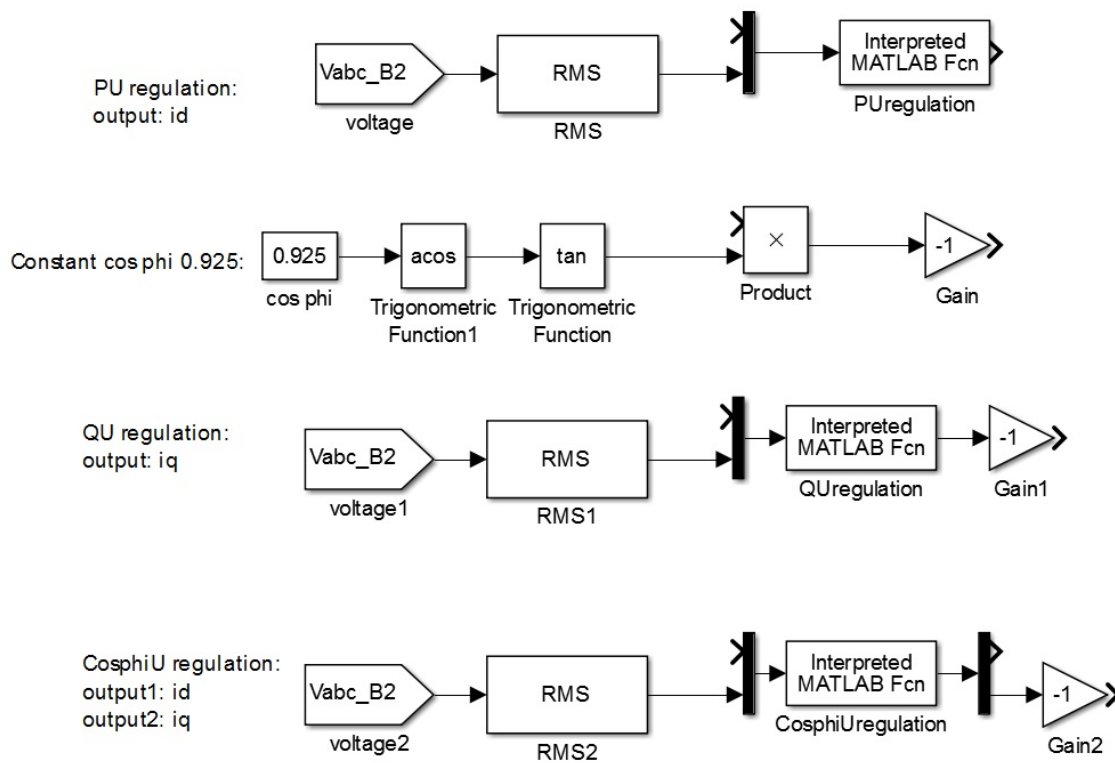


Figure 4.6: Inverter regulations

4.2 Analytical calculation of NDZs

Following section will describe analytical calculations of NDZ for each inverter regulation.

There are two possibilities for calculating the NDZ:

1. PV active and reactive power outputs are changed, while RLC load remains constant.
2. RLC load is changed, while PV active and reactive power outputs remain constant.

Possibility number 2 was chosen in the frame of this thesis, because changing the RLC load is much easier and less computationally difficult than changing active and reactive power outputs of PV. Another reason is, that PV outputs already have to be changed for each inverter regulation. Correlation of RLC load and output powers of PV can be explained with Equations 4.5 and 4.6. U_{RMS} is 25 kV in both equations, as already explained in one of the previous sections. Reference P_{PV} is 975 kW and reference Q_{PV} is 0 V Ar (reference case in this thesis is, when PV array inject only max active power into the grid). From the equations it can be concluded, that changing of resistive load is mainly responsible for voltage protection borders and changing of inductive and/or capacitive loads is mainly responsible for frequency protection borders.

$$P_{PV} = \frac{U_{RMS}^2}{R_{Load}} \quad (4.5)$$

$$Q_{PV} = U_{RMS}^2 * \left(\frac{1}{\omega * L_{Load}} - \omega * C_{Load} \right) \quad (4.6)$$

The reference RLC load values for the null or total matching point were calculated in the following. R load calculation is presented with equation 4.7. It is presumed, that all active power from the PV is consumed by the resistive load. For calculations of L and C loads additional assumptions have to be made. If PV has only active power output ($Q_{PV} = 0$ V Ar), then the relation between inductive and capacitive load can be described with Equation 4.8.

$$R_{Load} = \frac{U_{RMS}^2}{P_{PV}} \quad (4.7)$$

$$\frac{1}{\omega * L_{Load}} = \omega * C_{Load} \quad (4.8)$$

An infinite number of solutions is possible for L_{Load} and C_{Load} according to Equation 4.8, as long as $|Q_L| = |Q_C|$. In order to get the reference inductive and capacitive loads, they were calculated at exact $\cos\varphi_{Load} = 0.9$. This $\cos\varphi_{Load}$ was chosen, because it is the lowest possible power factor, that is tolerated from grid operator for residential users, according to [25]. Inductive and capacitive load were calculated with the following equations:

$$S_{Load} = \frac{P_{PV}}{\cos\varphi_{Load}} \quad (4.9)$$

$$Q_L = \sqrt{S_{Load}^2 - P_{PV}^2} \quad (4.10)$$

$$L_{Load} = \frac{U_{RMS}^2}{\omega * Q_L} \quad (4.11)$$

$$C_{Load} = \frac{Q_C}{\omega * U_{RMS}^2} \quad (4.12)$$

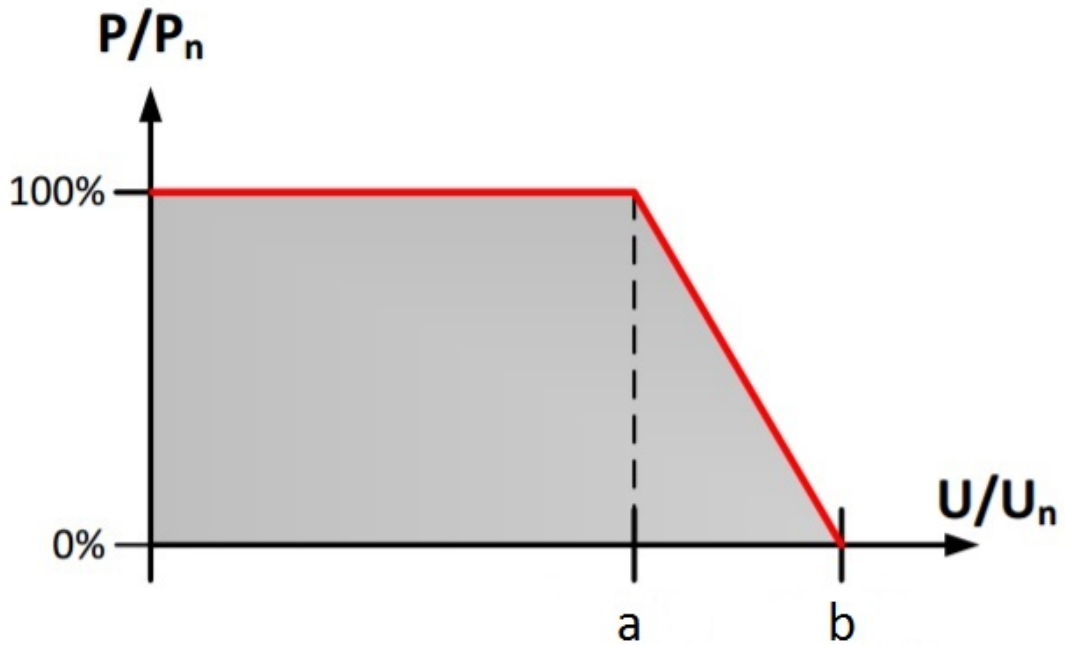
The calculated values for RLC load in null point are presented in Table 4.2. Calculations of further RLC values and consequently NDZ borders for different inverter regulations will be presented in detail in the following subsections. Only R and L loads were changed during analytical calculations and model simulations in order to get different mismatches between PV and load. If both, L and C loads would be changing, analytical calculation of NDZs could mathematically not be solved, because one equation would have two unknown variables. C load was therefore kept constant through all studies.

Table 4.2: RLC load values in null point

R load [Ω]	641.0256
L load [H]	4.2130
C load [μF]	2.4050

4.2.1 $P(U)$ inverter regulation

$P(U)$ inverter regulation was already described in one of the subsections of Chapter 3. For easier understanding, the regulation's statics is again depicted in Figure 4.7.

Figure 4.7: $P(U)$ inverter regulation statics

The figure shows, that active power output has to be regulated, once certain voltage point is exceeded. Grid operator chooses the appropriate regulating voltage points according to the situation on the grid. Voltage points presented in the Table 4.3 were chosen for this thesis's simulations and analytical calculations on the basis of [9].

Table 4.3: Voltage set points for $P(U)$ regulation

Point	Voltage $[\frac{U}{U_N}]$	Active power output $[\frac{P}{P_N}]$
a	110%	100%
b	112%	0%

Analytical calculation of the over/under voltage and frequency protection borders will be explained in the following, on the example of UVP and UFP borders. The whole process of calculating the NDZ borders is actually flipping of the basic two equations, which were

presented in subsection 4.2, Analytical calculation of NDZs. These Equations were 4.5 and 4.6. Firstly, the R load determination at under voltage point, at which protection should react and stop the injecting of the PV into the grid is presented with Equation 4.13. $factor_{UVP}$ is in this case 0.7 and was given in the Table 4.1. Furthermore, active power consumed by the calculated R load is calculated with Equation 4.14 and in the last step the actual border for chosen NDZ plotting is calculated with Equation 4.15.

$$R_{UVP} = \frac{(factor_{UVP} * U_{RMS})^2}{P_{PV}} \quad (4.13)$$

$$P_{LOAD,UVP} = \frac{(U_{RMS})^2}{R_{UVP}} \quad (4.14)$$

$$UVP = P_{LOAD,UVP} - P_{PV} \quad (4.15)$$

UFP border calculation is very similar. Firstly, the L load determination at under frequency point, at which protection should react and stop injecting of PV into the grid, is presented with Equation 4.16. f_{UFP} is in this case 47.5 Hz and was given in the Table 4.1. Reactive power of this load is calculated in Equation 4.17 and the actual NDZ border in Equation 4.18. C load is kept constant throughout all calculations, like already mentioned in previous subsection.

$$L_{UFP} = \frac{1}{(2 * \pi * f_{UFP})^2 * C_{load}} \quad (4.16)$$

$$Q_{LOAD,UFP} = U_{RMS}^2 * \left(\frac{1}{2 * \pi * f_N * L_{UFP}} - 2 * \pi * f_N * C_{load} \right) \quad (4.17)$$

$$UFP = Q_{LOAD,UFP} - Q_{PV} \quad (4.18)$$

Same procedures are used to calculate all borders of NDZ for $P(U)$ inverter regulation. NDZ limits in numerical form for this inverter regulation are collected in Table 4.4. The collected NDZ area is depicted in Figure 4.8. Green lines represent OFP and UFP, while blue lines represent OVP and UVP. Green-blue rectangle presents the standard NDZ area with only active power output of inverter. The red rectangle on the left presents additional NDZ area, because of $P(U)$ regulation. This area and its voltage protection borders were calculated on the same basic principle as already described in previous paragraphs. The

4 Analytical background

calculation was done for 1000 voltage points from point a ($100\% \frac{U}{U_N}$) to point b ($110\% \frac{U}{U_N}$). It was done in a for loop. Frequency protection borders for this area were kept the same as for standard area (on the right side), because it was analytically found out, that based on previous equations, $P(U)$ inverter regulation should not affect frequency protection borders.

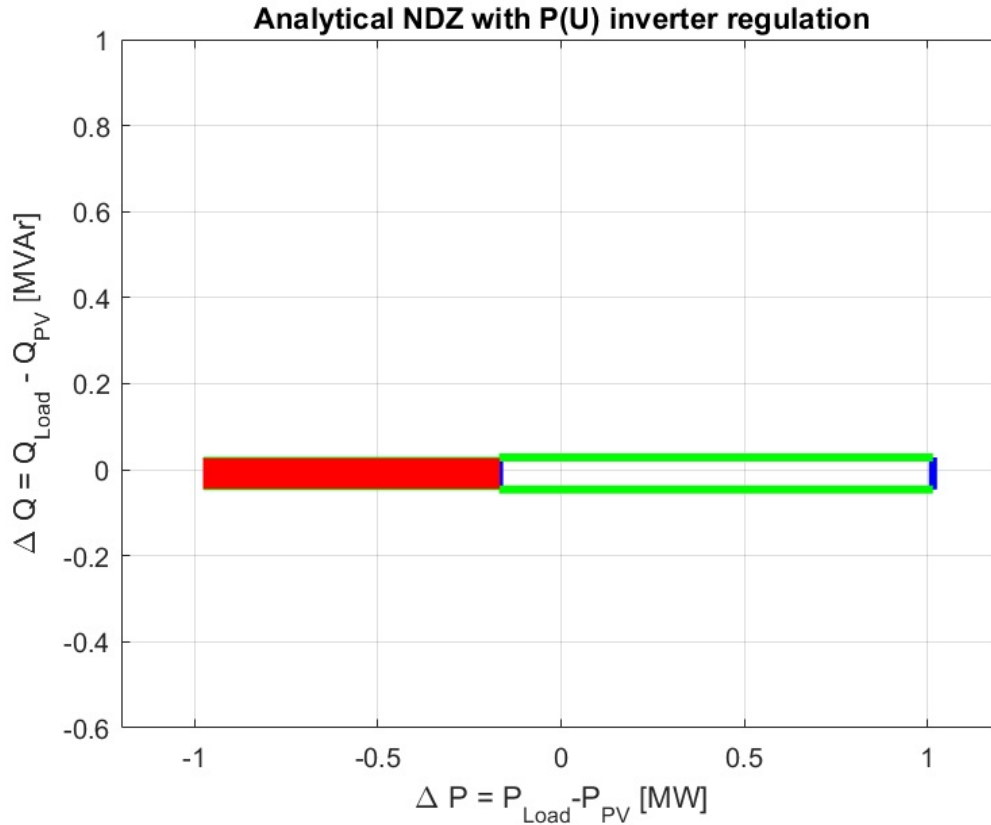


Figure 4.8: Analytical NDZ with $P(U)$ inverter regulation

4.2.2 $P(U) + \text{constant } \cos\varphi_{PV} = 0.925$ over excited inverter regulation

$P(U)$ with constant $\cos\varphi_{PV} = 0.925$ over excited inverter regulation was introduced in addition to standard $P(U)$ regulation. The reason for a mixed regulation lies especially in observation of frequency protection limits, since those limits were constant with $P(U)$ inverter regulation. The proposed mixture could offer an insight of how the NDZ changes if additional reactive power injection from the PV is proposed.

Table 4.4: NDZ borders for $P(U)$ inverter regulation

Protection	Set value	NDZ borders [MW] or [MVA _r]
Under-voltage protection	$0.7 * U_N$	1.015
Over-voltage protection	$1.1 * U_N$	-0.169
Over-voltage protection, $P(U)$ area	/	-0.975
Over-frequency protection	51.5 Hz	0.029
Under-frequency protection	47.5 Hz	-0.046

With the given $\cos\varphi_{PV}$, the equation for L load changes. Differences emerge, because Q_{PV} is consequentially no longer 0. Instead, PV inject reactive power into the grid. New calculation of L load on an example of under frequency protection at under voltage is presented with Equation 4.19. Other equations (4.17 and 4.18) in the process of frequency protection limit calculation remain the same.

$$L_{UFP \text{ at } UVP} = \frac{1}{2 * \pi * f_{UFP}} * \frac{1}{\frac{Q_{PV}}{(factor_{UVP} * U_{RMS})^2} + 2 * \pi * f_{UFP} * C_{load}} \quad (4.19)$$

All numerical values of NDZ borders are collected in the Table 4.5. If comparison is done with Table 4.4, where NDZ limits for standard $P(U)$ regulation are presented, it can be concluded that voltage protection borders remain the same, while frequency protection borders change.

Easier comparison of both regulation can be done by looking at Figure 4.9. Green lines represent frequency protection borders, while blue lines represent voltage protection borders. Red area on the left is presentation of the additional NDZ, because of P(U) inverter regulation. This area was again determined in for loop, for 1000 points from point a (100% $\frac{U}{U_N}$) to point b (110% $\frac{U}{U_N}$). Voltage protection and under and over frequency protection limits were calculated for every point in the for loop.

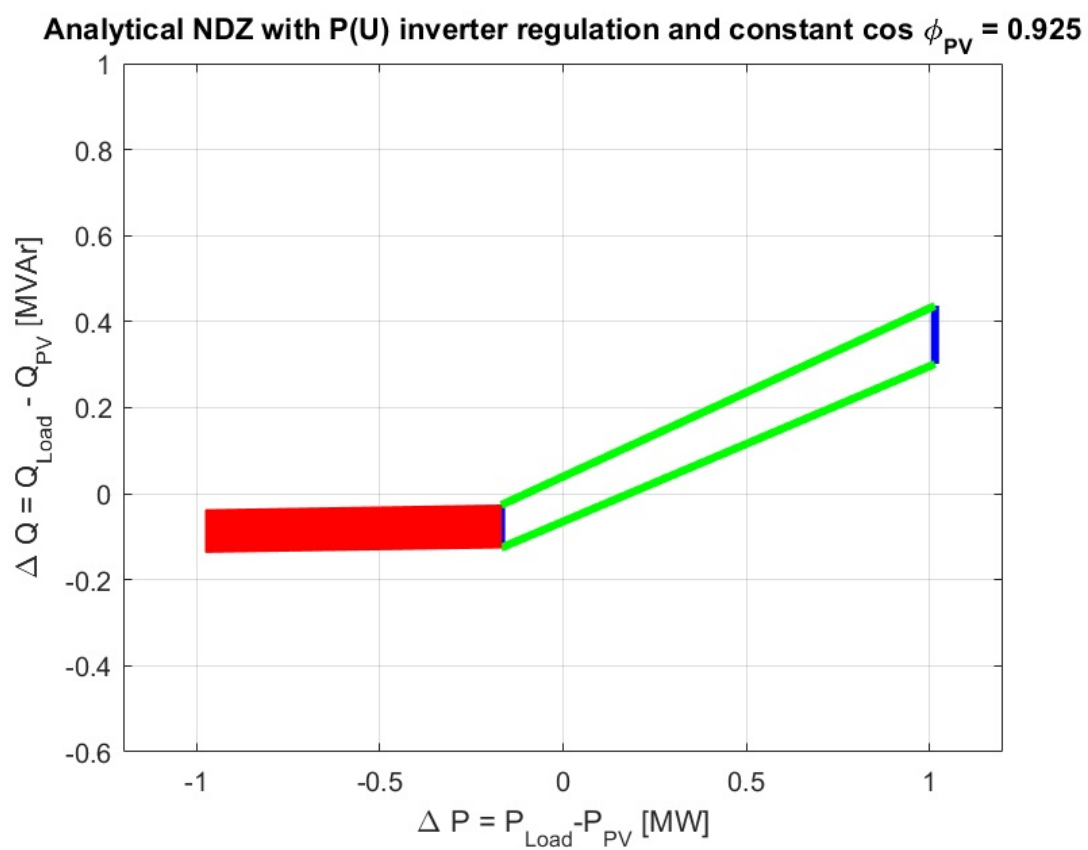


Figure 4.9: Analytical NDZ with $P(U) + \text{constant } \cos \phi_{PV} = 0.925$ over excited inverter regulation

Table 4.5: NDZ borders for $P(U) + \text{constant } \cos\varphi_{PV} = 0.925$ over excited inverter regulation

Protection	Set value	NDZ borders [MW] or [MVar]
Under-voltage protection	$0.7 * U_N$	1.015
Over-frequency at under-voltage protection	51.5 Hz; $0.7 * U_N$	0.437
Under-frequency at under-voltage protection	47.5 Hz; $0.7 * U_N$	0.302
Over-voltage protection	$1.1 * U_N$	-0.169
Over-frequency at over-voltage protection	51.5 Hz; $1.1 * U_N$	-0.026
Under-frequency at over-voltage protection	47.5 Hz; $1.1 * U_N$	-0.126
Over-voltage protection, $P(U)$ area	/	-0.975
Over-frequency at over-voltage protection, $P(U)$ area	/	-0.038
Under-frequency at over-voltage protection, $P(U)$ area	/	-0.136

4.2.3 $Q(U)$ inverter regulation

Main features of $Q(U)$ inverter regulation were already presented in Chapter 3. The regulation statics is again depicted in Figure 4.10. This regulation ensures certain reactive power outputs at certain voltage points in order to provide grid stabilization at under/over voltages. For example: When voltage is high, inverter starts consuming reactive power and consequentially voltage is reduced. Voltage set points a, b, c and d and values of reactive power outputs at these set points for medium voltage grid were determined on basis of [9] and are collected in Table 4.6.

Table 4.6: Voltage set points for $Q(U)$ regulation

Point	Voltage $[\frac{U}{U_N}]$	Reactive power output $[\frac{Q}{S}]$
a	90%	38%
b	98%	0%
c	102%	0%
d	110%	-38%

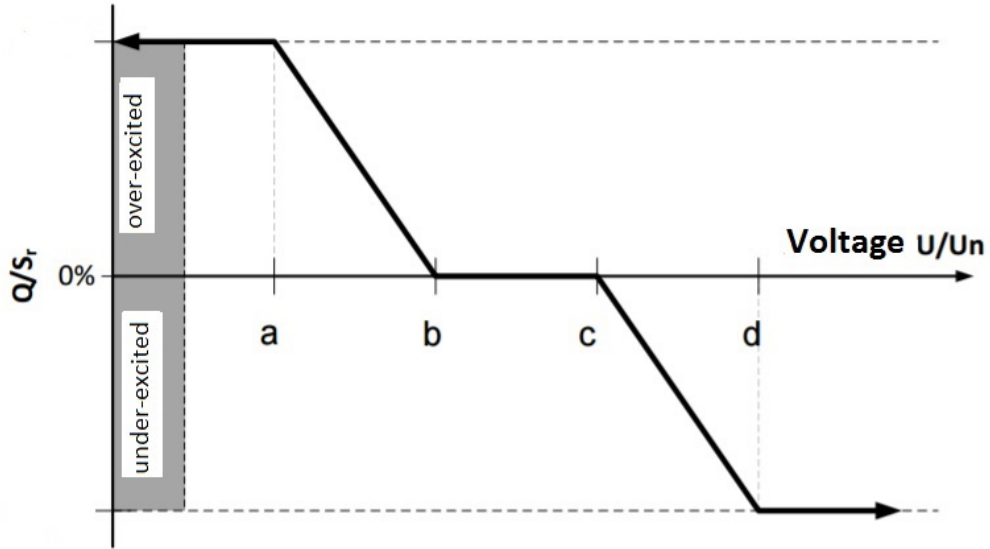


Figure 4.10: $Q(U)$ inverter regulation statics

Analytical calculation of NDZ for $Q(U)$ regulation was done separately for different areas. The final outcome is presented in Figure 4.11. Green lines in the figure represent frequency protection borders, while blue lines represent voltage protection borders. NDZ can be divided in four areas:

1. **Rectangle in the middle:** This rectangle represents “b-c” area from the regulation statics. Reactive power output of PV is in this case zero and borders of voltage and frequency protection functions were gathered with Equations 4.13 - 4.18. Numerical values of protection limits are gathered in Table 4.7.

Table 4.7: NDZ borders for $Q(U)$ inverter regulation, rectangle in the middle

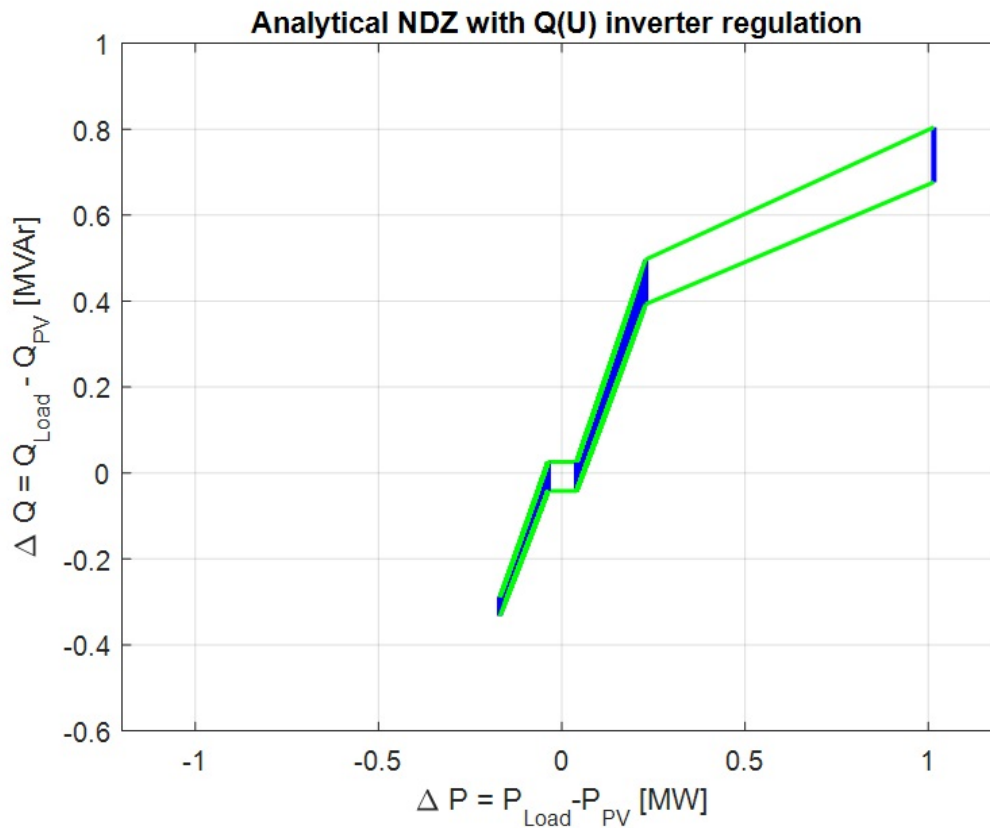
Protection	Set value	NDZ borders [MW] or [MVar]
Under-voltage protection	$b * U_N$	0.040
Over-voltage protection	$c * U_N$	-0.038
Over-frequency protection	51.5 Hz	0.029
Under-frequency protection	47.5 Hz	-0.046

2. **Shape on the left of the rectangle:** This shape represents “c-d” area from the

regulation statics. Since reactive power output in this area is changing according to voltage, example of L loads calculation for NDZ is presented with Equation 4.19. Same equations as in point 1 were used for other calculations of NDZ borders. The calculation was done for 1000 voltage points from point c, $102\% \frac{U}{U_N}$ to point d, $110\% \frac{U}{U_N}$ in for loop. Numerical values of protection limits are gathered in Table 4.8.

Table 4.8: NDZ borders for $Q(U)$ inverter regulation, shape on the left of the rectangle

Protection	Set value	NDZ borders [MW] or [MVar]
Over-voltage protection	$d * U_N$	-0.169
Over-frequency at over-voltage protection	51.5 Hz; $d * U_N$	-0.287
Under-frequency at over-voltage protection	47.5 Hz; $d * U_N$	-0.337

Figure 4.11: Analytical NDZ with $Q(U)$ inverter regulation

4 Analytical background

3. **Shape on the right of the rectangle:** This shape represents “a-b” area from the regulation statics. The calculations were done in the same way as for point 2. Numerical values of protection limits are gathered in Table 4.9.

Table 4.9: NDZ borders for $Q(U)$ inverter regulation, shape on the right of the rectangle

Protection	Set value	NDZ borders [MW] or [MVar]
Under-voltage protection	$a * U_N$	0.229
Over-frequency at under-voltage protection	51.5 Hz; $a * U_N$	0.500
Under-frequency at under-voltage protection	47.5 Hz; $a * U_N$	0.389

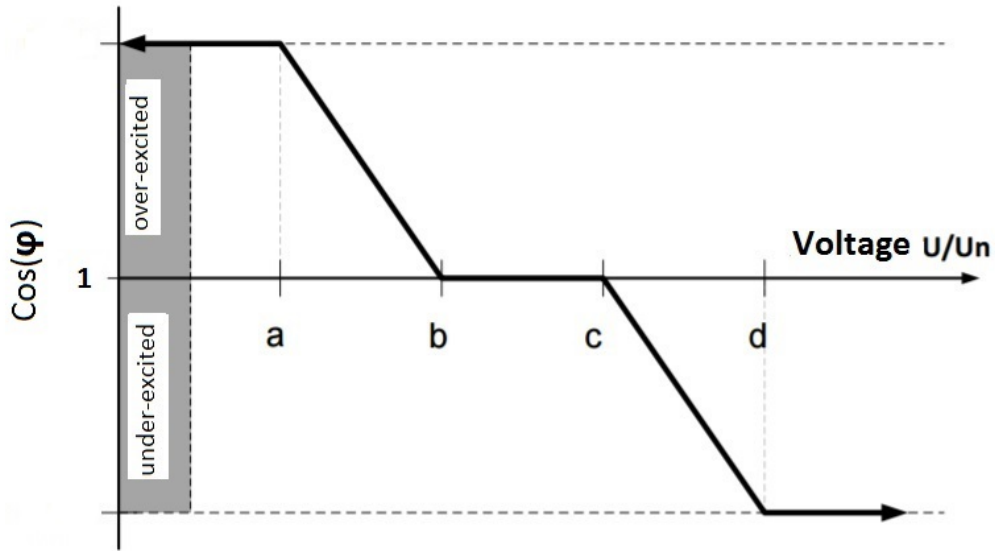
4. **Shape on the far right:** This shape represents area “a-UVP point”. Numerical values of protection limits are gathered in Table 4.10.

Table 4.10: NDZ borders for $Q(U)$ inverter regulation, shape on the far right

Protection	Set value	NDZ borders [MW] or [MVar]
Under-voltage protection	$0.7 * U_N$	1.015
Over-frequency at under-voltage protection	51.5 Hz; $0.7 * U_N$	0.808
Under-frequency at under-voltage protection	47.5 Hz; $0.7 * U_N$	0.672

4.2.4 $\cos\varphi(U)$ inverter regulation

Analytical NDZ of $\cos\varphi(U)$ inverter regulation will be presented in the following subsection. Statics of the proposed inverter regulation is presented in Figure 4.12. It was made on the basis of parametrization of PV inverters done by Salzburg Netz GmbH, [10]. $\cos\varphi(U)$ inverter regulation ensures adjusted active and reactive power outputs of PV, once certain voltage points are exceeded. So, in comparison to $Q(U)$ regulation, this regulation does not support maximal yield for DER, but can be potentially useful for improved grid stability. In terms of NDZ, a bit bigger NDZ is expected, since changing of active power output offers additional “protection”. Voltage set points and power factors collected in Table 4.11 were chosen in a meaningful way, because [9] does not specify exact set points for this regulation.

Figure 4.12: $\cos\varphi(U)$ inverter regulation staticsTable 4.11: Voltage set points for $\cos\varphi(U)$ regulation

Point	Voltage [$\frac{U}{U_N}$]	Power factor [$\cos\varphi$]
a	90%	0.925 over-excited
b	98%	1
c	102%	1
d	110%	0.925 under-excited

Analytical NDZ with $\cos\varphi(U)$ inverter regulation is presented in 4.13. As expected, the shape is very similar to the one gathered with $Q(U)$ inverter regulation, Figure 4.11. Green lines represent frequency protection borders, while blue lines represent voltage protection borders. Figure 4.13 can be misunderstood, because green lines as frequency protection borders should only be on the outside of the NDZ area. Instead, there are some areas in the figure, which are filled with green color. The explanation for this lies in Figure 4.14, where NDZ with $\cos\varphi(U)$ inverter regulation is calculated in for loops with only 3 steps (NDZ in Figure 4.13 is calculated in for loops with 1000 steps). Voltage protection borders

4 Analytical background

for each point are shifted in a way, that when calculation is done for 1000 points these areas get filled with green colour. In conclusion, the problem lies in the way of depiction, frequency protection borders are however still only on the outside.

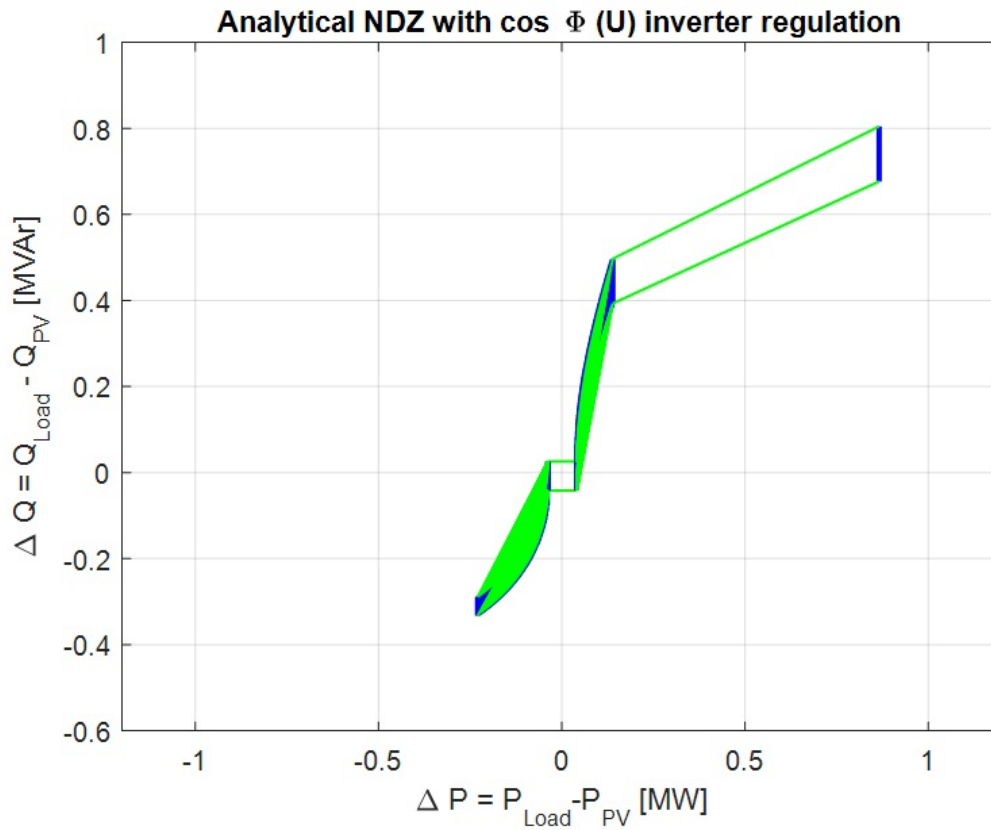


Figure 4.13: Analytical NDZ with $\cos\varphi(U)$ inverter regulation

NDZ can again be divided into four areas. Calculations for each area were done in the same way and with the same equations as described in the previous section for $Q(U)$ inverter regulation. Different active power outputs are responsible for slightly different shapes in the analytical NDZ.

1. **Rectangle in the middle:** The rectangle in the middle has exactly the same characteristics as with the $Q(U)$ inverter regulation. Numerical values of protection borders for this area can therefore be found in Table 4.7.
2. **Shape on the left of the rectangle:** This area represents “c-d” area on the

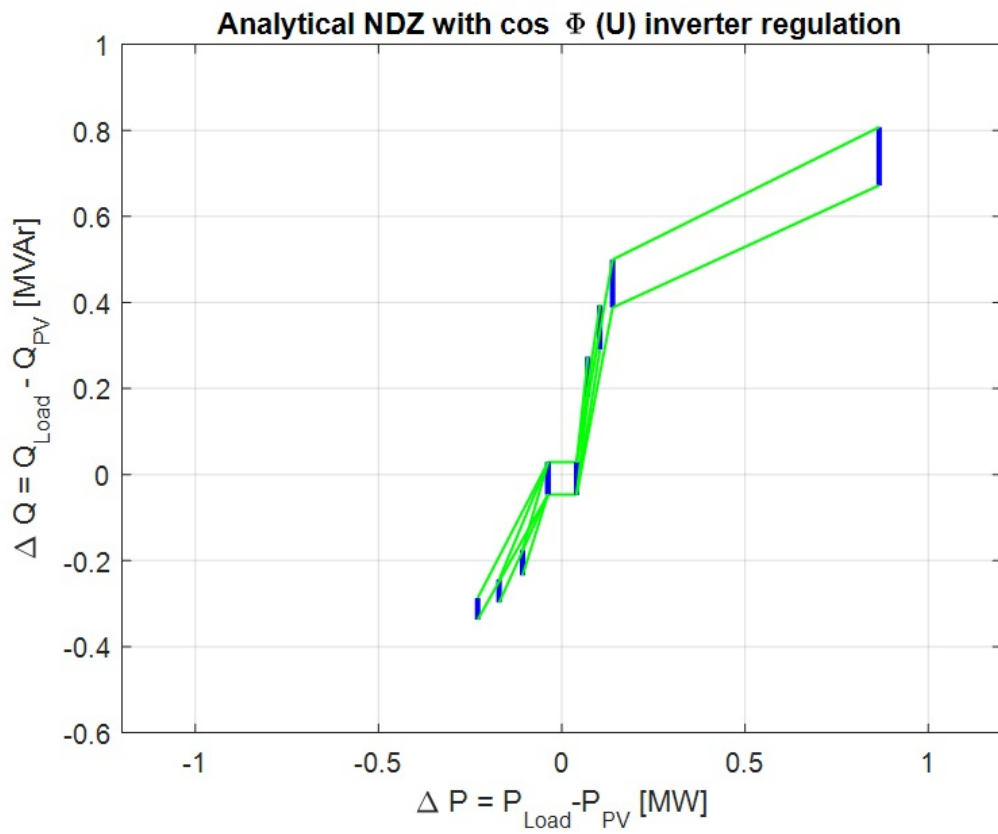


Figure 4.14: Explanation of green filled areas from Figure 4.13

4 Analytical background

inverter regulation statics. Numerical protection limits are collected in Table 4.12.

Table 4.12: NDZ borders for $\cos\varphi(U)$ inverter regulation, shape on the left of the rectangle

Protection	Set value	NDZ borders [MW] or [MVA _r]
Over-voltage protection	$d * U_N$	-0.230
Over-frequency at over-voltage protection	51.5 Hz; $d * U_N$	-0.287
Under-frequency at over-voltage protection	47.5 Hz; $d * U_N$	-0.337

3. Shape on the right of the rectangle: This area represents “a-b” area on the inverter regulation statics. Numerical protection limits are collected in Table 4.13.

Table 4.13: NDZ borders for $\cos\varphi(U)$ inverter regulation, shape on the right of the rectangle

Protection	Set value	NDZ borders [MW] or [MVA _r]
Under-voltage protection	$a * U_N$	0.138
Over-frequency at under-voltage protection	51.5 Hz; $a * U_N$	0.500
Under-frequency at under-voltage protection	47.5 Hz; $a * U_N$	0.389

4. Shape on the far right: This shape represents area “a-UVP point”. Numerical values of protection limits are gathered in Table 4.14.

Table 4.14: NDZ borders for $\cos\varphi(U)$ inverter regulation, shape on the far right

Protection	Set value	NDZ borders [MW] or [MVA _r]
Under-voltage protection	$0.7 * U_N$	0.866
Over-frequency at under-voltage protection	51.5 Hz; $0.7 * U_N$	0.808
Under-frequency at under-voltage protection	47.5 Hz; $0.7 * U_N$	0.672

If numerical values of protection borders were compared to values with $Q(U)$ inverter regulation, it could be concluded that voltage protection borders change, as a consequence of active power output change. Frequency protection limits remain the same, but only in

the set points, because the reactive power output of the inverter at $\frac{Q}{S} = 0.38$ is the same as at $\cos\varphi = 0.925$. Frequency protections limits between the set points are diverging, as can be seen, if both figures are compared (4.11 and 4.13). Further comments of the NDZs will be done in the Chapter 5, where NDZs gathered with simulation model will be presented.

5 Results and analysis

The following chapter starts with the explanation of the course of Simulink model simulation. Furthermore, simulated NDZs for different inverter regulations are presented and compared with analytical acquired NDZs. Transition behaviour of frequency and voltage in process from grid connected mode to island mode are looked at. As an addition, certain Simulink model parameters are tested in order to measure model's efficiency and speed. NDZ with changed parameters is presented and compared to NDZ with basic parameters. One of the proposed inverter regulations is chosen and researched further into detail with appropriate additions, based on combined knowledge on different NDZs, dynamic behaviour of frequency and voltage and model efficiency.

5.1 The course of simulation

Basic Simulink model elements are PV array, boost converter, inverter, filter, transformer, RLC Load, switch and slack bus, as already explained in Chapter 4, Figure 4.1. The run time of simulation is 2 s, the switching time (transition from grid to island mode) is at 0.5s. First 0.5s of the time is needed for the stabilization of the system, because PV array needs some time before it starts to inject required active and reactive power into the grid. Switch is closed during this time and slack bus is connected to other parts of the model. Voltage and frequency are therefore in the first 0.5s mainly influenced from slack bus and are almost constant at $U_{RMS, phase-to-phase} = 25$ kV and $f = 50$ Hz. After 0.5 s switch opens and slack bus is not connected any more. This is the transition from grid to island mode. Frequency and voltage are in island mode mainly dependent on the match between PV array output and parallel RLC load. Transition period will be precisely looked at in one of the following sections.

5 Results and analysis

The acquire of NDZs was done with the so called “space sweep”. Model was run in the MATLAB script in two for loops. Outer loop was used for changing R load parameter and the inner for changing L load parameter. C load was kept constant, as already explained in Chapter 4. For easier understanding of the space sweep, Figure 5.1 should be looked at. Standard zone (NDZ with only active power output) was recorded in this figure.

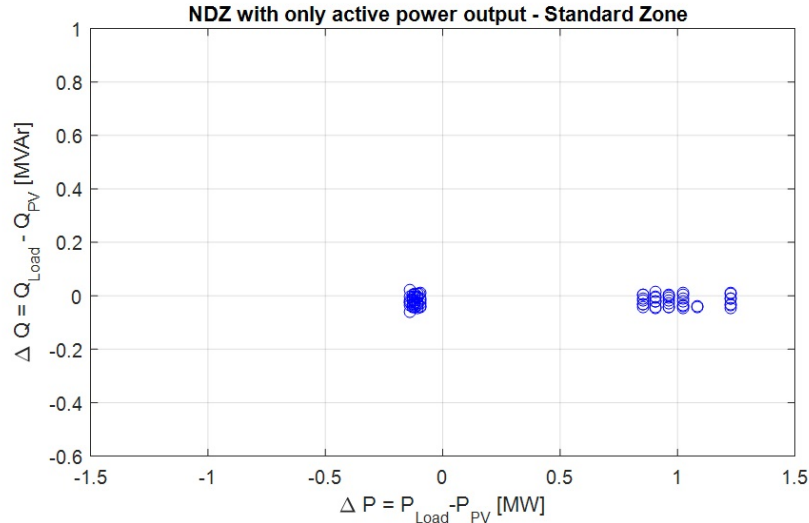


Figure 5.1: NDZ with only active power output - Standard Zone

The space sweep in this case was done in two parts and parameters can be found in Table 5.1. Parameters were chosen on basis of analytical calculation with appropriate deviation in a way, that none of starting and finishing parameters of R and L loads was detected as NDZ. Number of steps for each load parameter in the table is the number of steps in for loop in MATLAB script. Part 1 was used for finding UVP border - right part of blue circles in the Figure 5.1 and part 2 was used for finding OVP border - left part of blue circles in the Figure 5.1. For example: at $R_{load} = 350 \Omega$, (far left column of blue circles among part 1 space sweep on the right) NDZ was recorded at approximately five L load points. Other fifteen L load points at $R_{load} = 350 \Omega$ were marked as detection zone and can therefore not be seen in the figure. The space between part 1 and 2 was not swept, because it was analytically found out, that frequency borders should remain practically unchanged throughout the whole area and additional sweep was not needed. Bigger areas had to be swept for further inverter regulations (more in the following section), because

analytically gathered results could not be sufficient indicator, that Simulink model would offer similar results.

Table 5.1: Parameters for space sweep of standard zone

Parameter	Part 1	Part 2
R load start	250 Ω	750 Ω
R load finish	350 Ω	850 Ω
R load steps	10	10
L load start	4 H	4 H
L load finish	6 H	6 H
L load steps	20	20

The standard NDZ area was furthermore adapted in program Inkscape, Figure 5.2. Inkscape offers user the possibility to manually draw the line around wanted points and fill up the whole covered space.

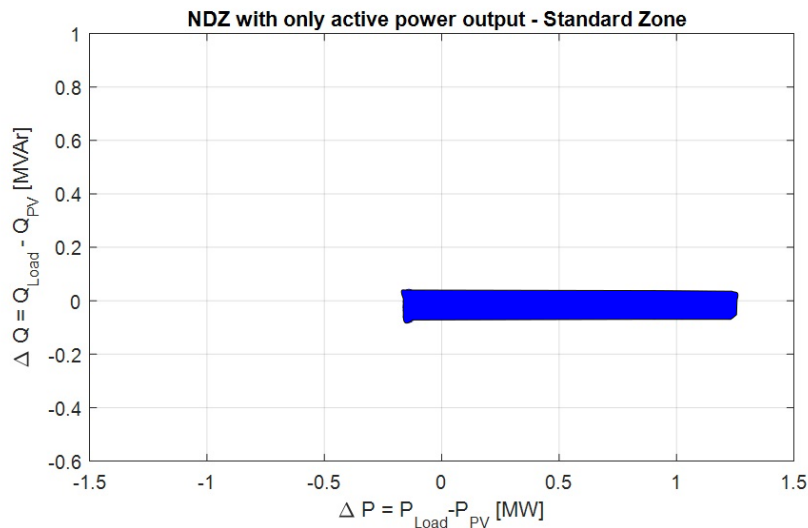


Figure 5.2: NDZ with only active power output - Standard Zone, adapted with Inkscape

Figure 5.3 offers the comparison of the analytical and simulated NDZ areas. As can be

5 Results and analysis

seen, the simulated area is a bit broader. The biggest difference is however in UVP border (on the right), where simulated area is moved towards right for approximately 0.2 MW. The reason for the shift could lie in the behaviour of the voltage after transition. Voltage after transition from grid to island mode does not instantly fall/rise to the specific value and stay constant, as was assumed in analytical calculation. The movement is rather oscillated (transient behaviour) and this could be the reason for shift.

In addition, it has to be noted, that recording of UVP border of standard NDZ was a bit unusual. In Figure 5.1, it can be seen on the right, that UVP border was recorded at some R load point for several L load points. But at the next R load point only one L load point was detected as NDZ point, which is unexpected. It was expected, that at each of the next R load points, similar L load points would be detected as NDZ, because frequency protection borders should be constant for Standard Zone.

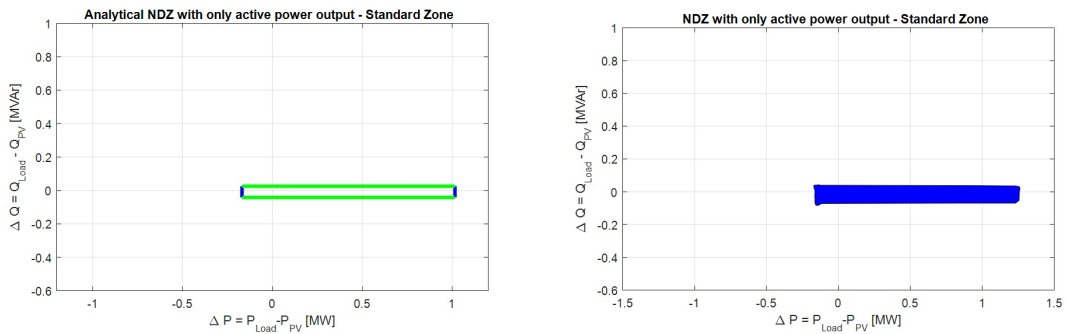


Figure 5.3: Comparison of analytical and simulated NDZs with only active power output - Standard Zone

5.2 Simulated NDZs

5.2.1 $P(U)$ inverter regulation

Based on analytical calculation of NDZ with $P(U)$ inverter regulation, parameters in Table 5.2 were chosen for space sweep. Part 1 was used for the sweep of the whole area and part 2 was additional sweep in order to find precise UVP border. Observation of left figure of Figure 5.4 should be looked at in order to understand, why additional sweep for OVP border was not needed. It can be seen, that even though the R step remains the same

throughout the sweep, the higher the R load, the shorter is the spacing between recordings of NDZ. Therefore, it could be concluded, that OVP border was acquired precisely with part 1 of space sweep.

Table 5.2: Parameters for space sweep of $P(U)$ inverter regulation

Parameter	Part 1	Part 2
R load start	250 Ω	250 Ω
R load finish	2250 Ω	350 Ω
R load steps	70	10
L load start	4 H	4 H
L load finish	6 H	6 H
L load steps	20	20

Figure 5.4 shows the NDZ space sweep on the left and the NDZ adapted with Inkscape.

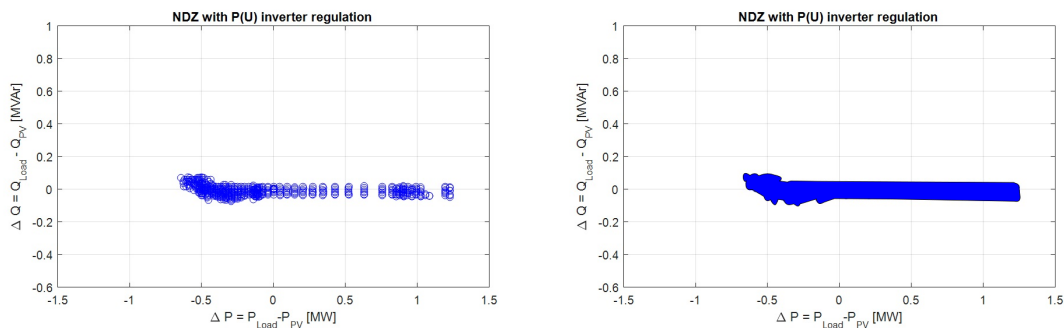


Figure 5.4: $P(U)$ inverter regulation: left - NDZ space sweep, right - NDZ adapted with Inkscape

The comparison of analytically acquired NDZ and simulated NDZ with $P(U)$ inverter regulation can be seen in Figure 5.5. Shapes of NDZs are very similar on the right side, simulated NDZ is only a bit broader. First big difference is the UVP border. UVP border at simulated NDZ is moved to the right for approximately 0.2 MW. The same shift occurred at standard zone in the previous section and the reasoning for this shift remains

5 Results and analysis

unclear.

Differences on the left side of the shapes can be seen at both, voltage and frequency protection borders. The reason for OVP at approximately -0.7 MW and not -0.975 MW can be explained with the way analytical calculation was done. Analytical calculation was done at ideal circumstances, transient behaviour (oscillations) was not taken into account. According to inverter regulation, active power output is drastically reduced as soon as voltage rises above $1.10\% U_N$. Looking at the Equations 4.13, 4.14 and 4.15, it can be seen, that when voltage is high, active power output is practically zero and R_{VP} in analytical calculation is therefore very big, $P_{LOAD,VP}$ goes towards null and voltage protection border is shifted towards maximum negative power output of PV - 975 kW. Circumstances in simulation are a bit different. Once certain voltage is exceeded, active power output is reduced, but as a consequence voltage also drops and active power should again be increased. The final effect is fluctuation of active power and voltage and the real OVP border is closer to the null point.

Frequency protection borders are in area of $P(U)$ inverter regulation not so “narrow” any more, because $P(U)$ regulation regulates the active power output. So, as soon as certain voltage is exceeded, active power is reduced and active power from load and PV are better matched. Frequency is better stabilized, when active power of PV and load are better matched and frequency protection does not trigger as quickly.

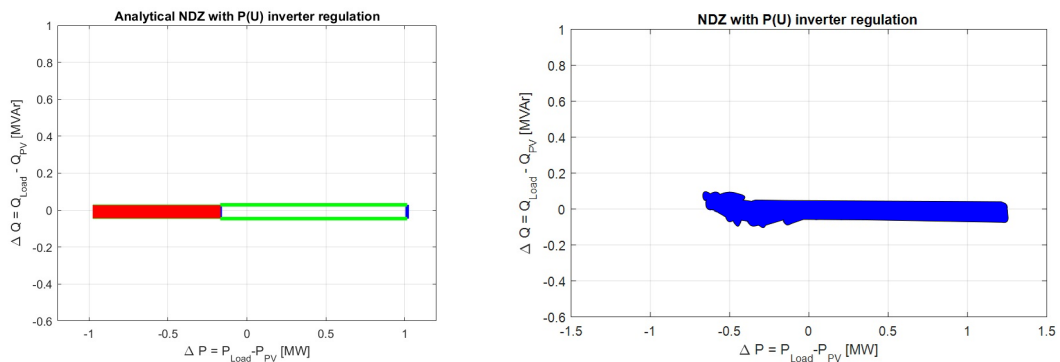


Figure 5.5: Comparison of analytical and simulated NDZs with $P(U)$ inverter regulation

5.2.2 $P(U) + \text{constant } \cos\varphi_{PV} = 0.925$ over excited inverter regulation

Parameters for space sweep with this regulation can be found in the Table 5.3. Parameters for part 1 were chosen based on analytical calculation. Other parts were chosen based on the observation of the gathered sweep and the level of missing knowledge on how the NDZ should look like at the “break” (area, where $P(U)$ regulation starts having impact). Part 2 and part 3 were therefore mainly for research of the “break”. Part 4 was needed for better determination of UVP border.

Table 5.3: Parameters for space sweep of $P(U) + \text{constant } \cos\varphi_{PV} = 0.925$ over excited inverter regulation

Parameter	Part 1	Part 2	Part 3	Part 4
R load start	250 Ω	700 Ω	720 Ω	250 Ω
R load finish	2250 Ω	800 Ω	750 Ω	350 Ω
R load steps	40	20	15	10
L load start	1 H	1.8 H	2 H	1 H
L load finish	3.5 H	2.8 H	2.5 H	2 H
L load steps	50	20	10	20

Figure 5.6 shows the NDZ space sweep on the left and the NDZ adapted with Inkscape.

Comparison of analytical and simulated NDZs is depicted in Figure 5.7. Right part of the figure is very similar at both NDZs. Simulated area is only a bit broader, which was already the case in previous comparisons of analytical and simulated NDZs. The interesting fact is, that UVP border lies at approximately 1 MW, so practically at the same point as in analytical calculation, which was not the case in previous gathered NDZ areas. Reasoning for this remains unclear.

NDZ area takes unexpected “jump” along y axes at approximately -0.1 MW, “break” area. Possible explanation for the “jump” could lie in the fluctuation of active power and voltage, because of $P(U)$ inverter regulation. Averaged voltage is therefore lower as it was

5 Results and analysis

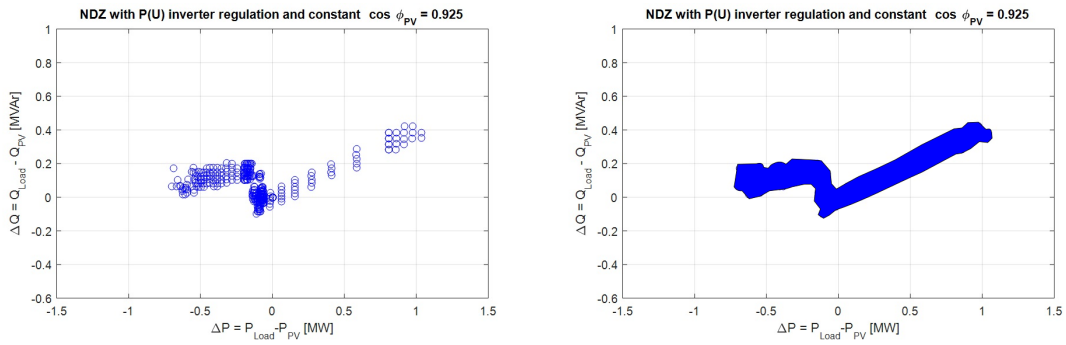


Figure 5.6: $P(U)$ + constant $\cos\phi_{PV} = 0.925$ inverter regulation: left - NDZ space sweep, right - NDZ adapted with Inkscape

in the area before -0.1 MW. Frequency protection borders at lower voltages are in case of $P(U)$ + constant $\cos\phi_{PV} = 0.925$ over excited inverter regulation detected at higher values, which is clearly seen in the Figure 5.7 on the right and can be also confirmed if Equations 4.19, 4.17 and 4.18 are studied. Effect of $P(U)$ regulation in connection with constant $\cos\phi_{PV} = 0.925$ over excited is therefore, that frequency protection borders in the regulated area are shifted up, so it is as though as inverter at -0.1 MW mismatch (where, $P(U)$ inverter regulation starts having impact) has similar frequency protection borders as at 0.35 MW.

The remaining left part of the NDZ has similar characteristics as it had with only $P(U)$ regulation. The explanation for difference in OVP borders between analytical and simulated NDZ was therefore already explained in previous subsection. Reasoning for broader frequency protection band was also offered in previous subsection.

5.2.3 $Q(U)$ inverter regulation

Parameters for space sweep of $Q(U)$ regulation are gathered in the Table 5.4. Values for part 1 and 2 were chosen on basis of analytical findings. These parts were separated, because it was unnecessary for part 1 to take so big L load area as in part 2. Part 3 offered additional sweep of the space, which was left rather empty after first two simulated areas.

Figure 5.8 shows the NDZ space sweep on the left and the NDZ adapted with Inkscape.

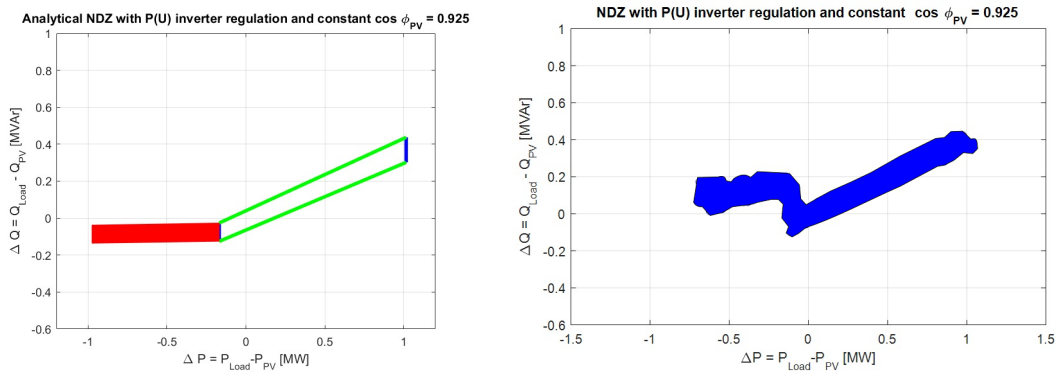


Figure 5.7: Comparison of analytical and simulated NDZs with $P(U) + constant cos \varphi_{PV} = 0.925$ inverter regulation

Table 5.4: Parameters for space sweep of $Q(U)$ inverter regulation

Parameter	Part 1	Part 2	Part 3
R load start	250 Ω	700 Ω	710 Ω
R load finish	750 Ω	850 Ω	720 Ω
R load steps	18	5	1
L load start	1.5 H	5 H	5 H
L load finish	5.5 H	25 H	15 H
L load steps	80	200	100

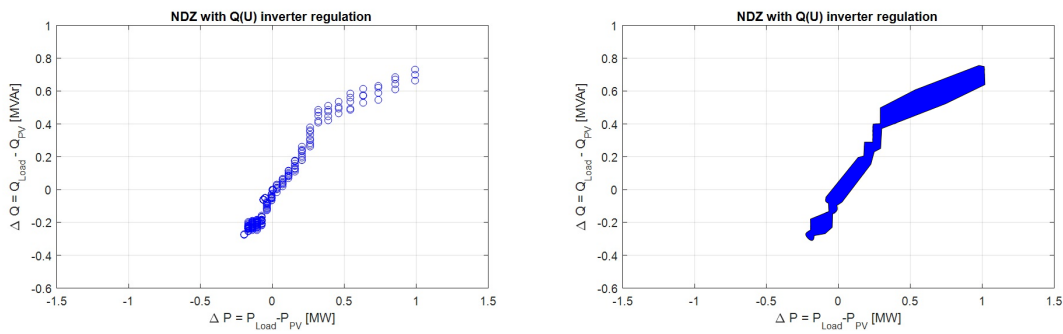


Figure 5.8: $Q(U)$ inverter regulation: left - NDZ space sweep, right - NDZ adapted with Inkscape

5 Results and analysis

Figure 5.9 offers comparison of analytical and simulated NDZs for $Q(U)$ inverter regulation. NDZ gathered with simulation is very similar to analytical one. UVP borders on the right and OVP borders on the left are practically the same. Simulated NDZ is however a bit broader in width throughout the whole area.

Biggest differences arise in transition areas (Figure 4.10: areas, where inverter changes its effect on outputs). Space sweep in transition areas detected kind of step transitions, which diverges from analytical result. For very precise result in transition areas, space sweep with really high resolution would be proposed.

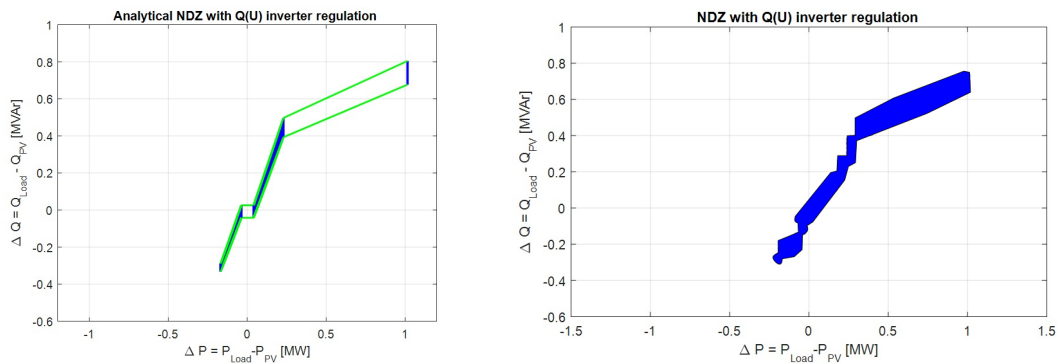


Figure 5.9: Comparison of analytical and simulated NDZs with $Q(U)$ inverter regulation

5.2.4 $\cos\varphi(U)$ inverter regulation

Parameters for space sweep of $\cos\varphi(U)$ regulation are gathered in the Table 5.5. Values for part 1 and 2 were chosen on analytical base in order to cover the whole potential NDZ area. Part 3 was additional sweep, because primary sweep was not sufficient in some areas to recognize the NDZ.

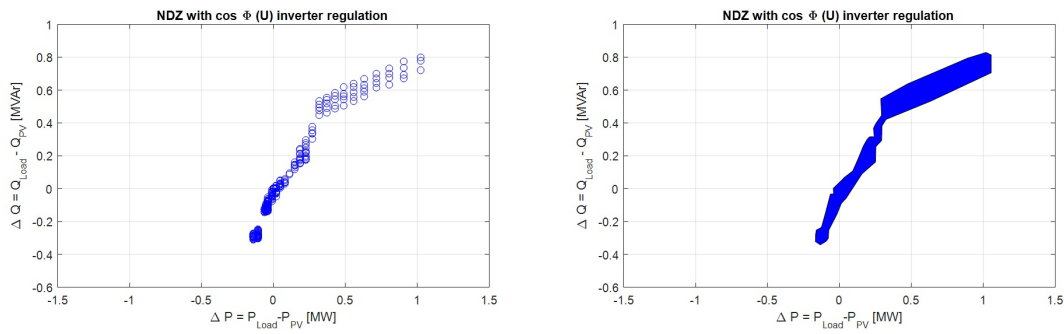
Figure 5.10 shows the NDZ space sweep on the left and the NDZ adapted with Inkscape.

Comparison of analytical and simulated NDZs with $\cos\varphi(U)$ inverter simulation is depicted in Figure 5.11. NDZs are very similar. The biggest difference arise at transition area at approximately 0.35 MW. Step transition is detected in this area, as was the case with $Q(U)$ inverter regulation and this diverges from analytical NDZ.

Comparison of simulated NDZs for $Q(U)$ and $\cos\varphi(U)$ inverter regulation brings the con-

Table 5.5: Parameters for space sweep of $\cos\varphi(U)$ inverter regulation

Parameter	Part 1	Part 2	Part 3
R load start	300 Ω	700 Ω	705 Ω
R load finish	700 Ω	850 Ω	725 Ω
R load steps	20	5	4
L load start	1.5 H	5 H	5 H
L load finish	5.5 H	15 H	15 H
L load steps	80	100	100

Figure 5.10: $\cos\varphi(U)$ inverter regulation: left - NDZ space sweep, right - NDZ adapted with Inkscape

5 Results and analysis

clusion, that $\cos\varphi(U)$ inverter regulation does not bring any special improvements in terms of NDZ. Namely, the NDZ is not smaller and is therefore not preferred for protection of the island. Based on this fact, $\cos\varphi(U)$ inverter regulation is not recognized as meaningful in comparison to $Q(U)$ regulation, because it also does not bring maximal economic yield for the PV unit (active power output is reduced in certain voltage areas).

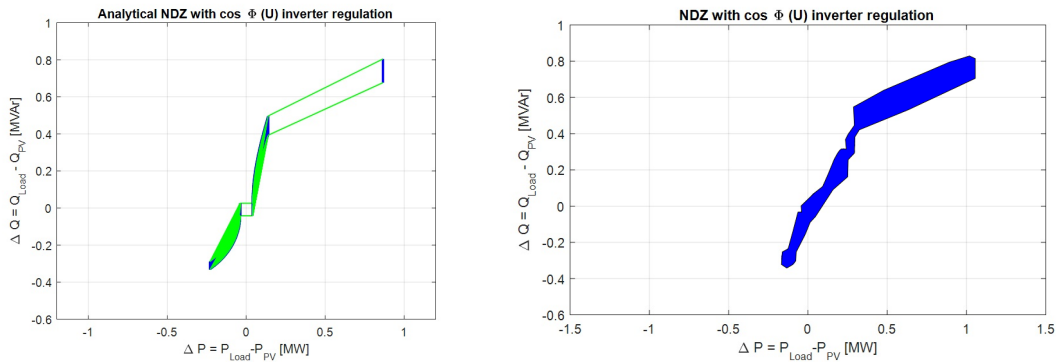


Figure 5.11: Comparison of analytical and simulated NDZs with $\cos\varphi(U)$ inverter regulation

5.3 Transition from grid mode to island mode

Dynamic behaviour of frequency and voltage during the transition period from grid to island mode is observed in the following section. Three random points within NDZ were chosen for each studied inverter regulation and courses of frequency and voltage were recorded. Conclusions were done based on gatherings, whether dynamic behaviour of frequency or voltage is potentially suitable for introduction of any new anti-islanding protection methods.

5.3.1 $P(U)$ inverter regulation

Figure 5.12 depicts three chosen points within NDZ, where behaviour of frequency and voltage was recorded. Transition 1 was recorded in the right point on the figure, transition 2 in the middle point and transition 3 in the left point. Points were chosen in a way to cover as much area of NDZ as possible.

5.3 Transition from grid mode to island mode

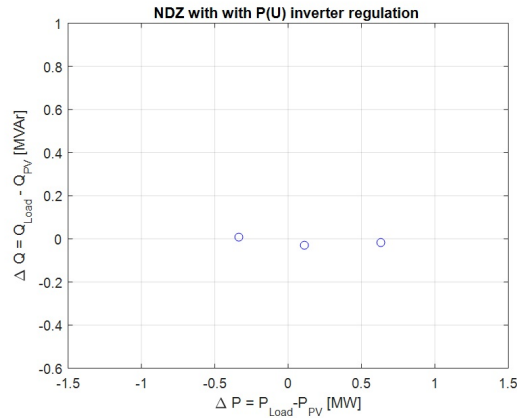


Figure 5.12: $P(U)$ inverter regulation: Transition points. Transition 1 right, transition 2 middle, transition 3 left

Three chosen transitions can be seen in Figure 5.13. Transition 1 is in the figure above, transition 2 in the middle and transition 3 below.

Frequency and voltage are constant at 50 Hz and 25 kV in the first 0.5 s of the simulation - grid mode. At 0.5 s switch opens and frequency and voltage experience certain oscillations, in order to try and maintain stability of the island.

Voltage in the first two transitions oscillates a lot in the first 0.1 s, 0.2 s after formation of the island. After that period, the approximate stability value is slowly found and voltage oscillates only a little. However, in the transition 3, voltage oscillates throughout the whole period from 0.5 s to end of simulation time at 2 s. Reason for this lies in $P(U)$ inverter regulation - transition 3 lies in the area, where $P(U)$ inverter regulation was already having effect. As already mentioned in the previous section, as soon as certain voltage point is exceeded, active power is reduced and as a consequence voltage drops - when such behaviour repeats itself it results in voltage fluctuation.

Transitions of frequency shows the biggest jump of frequency at 0.5 s - at the transition from grid to island mode. Especially jump in transition 2 is very big - $\frac{1.5 \text{ Hz}}{0.5 \text{ s}}$, which is explainable if Figure 5.12 is looked at. Transition 2 - point in the middle, is the most distant point from 0 on y axes (reactive power mismatch).

In conclusion, ROCOF method would be potentially appropriate and would make the NDZ narrower (ROCOF would theoretically only have an impact on width - frequency

5 Results and analysis

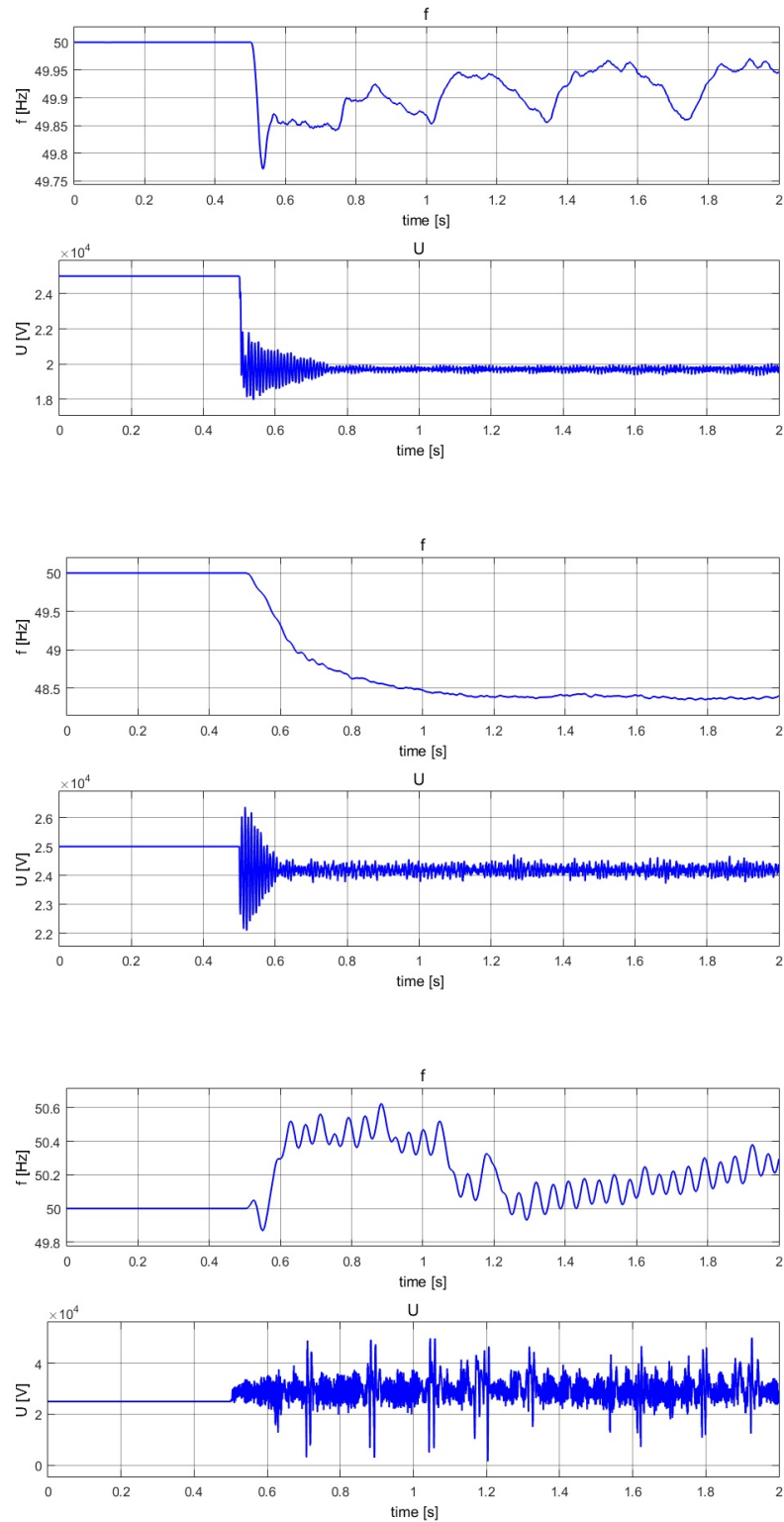


Figure 5.13: $P(U)$ inverter regulation: Frequency and voltage in transition from grid to island mode. Transition 1 above, transition 2 middle, transition 3 below

protection borders of the NDZ and not on the length - voltage protection borders), if the right settings would be introduced.

5.3.2 $P(U) + \text{constant } \cos\varphi_{PV} = 0.925$ over excited inverter regulation

Figure 5.14 depicts three chosen points within NDZ, where behaviour of frequency and voltage was recorded. Transition 1 was recorded in the right point on the figure, transition 2 in the middle point and transition 3 in the left point.

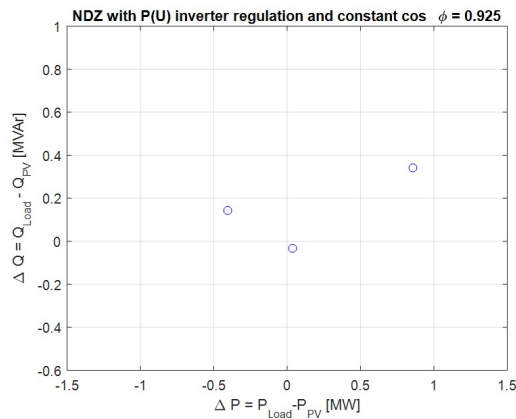


Figure 5.14: $P(U) + \text{constant } \cos\varphi = 0.925$ over excited inverter regulation: Transition points. Transition 1 right, transition 2 middle, transition 3 left

Chosen transitions can be seen in Figure 5.15. Behaviour of voltage in the three chosen points within NDZ with $P(U) + \text{constant } \cos\varphi_{PV} = 0.925$ over excited inverter regulation is similar to behaviour with only $P(U)$ regulation. Namely, voltage oscillates a lot right after island formation and then finds its stability value. Oscillations however maintain throughout the whole simulation in the transition 3, where voltage oscillates because of active power fluctuation.

Behaviour of frequency is also similar as in previous subsection. The biggest jumps of frequency happen in the first 0.5 s after island forming. Frequency experiences only small deviations after that. Frequency jumps are smaller in comparison to previous subsection, which is because of the transition points chosen. If points closer to frequency protection borders would be chosen for observation, frequency jumps would be bigger.

5 Results and analysis

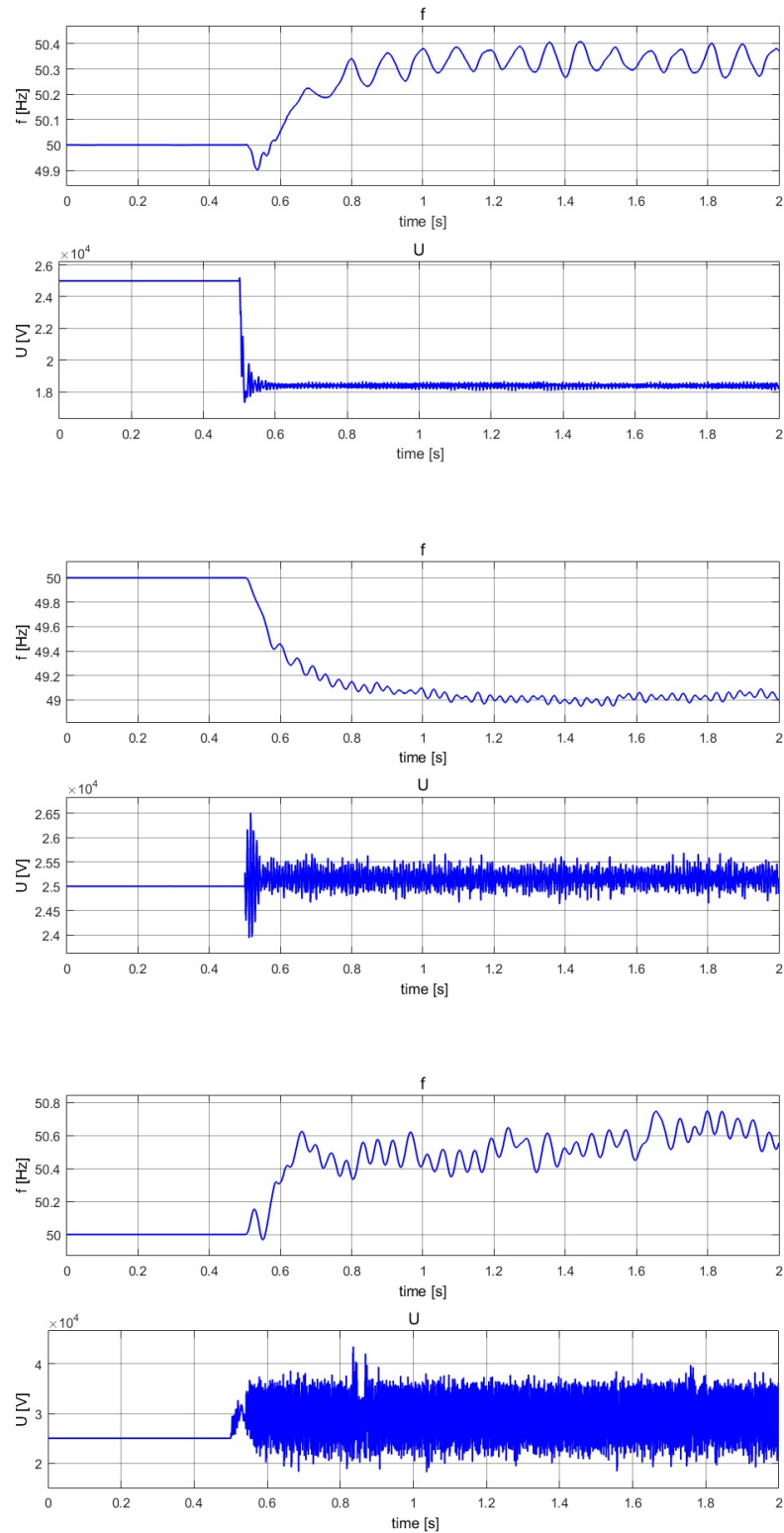


Figure 5.15: $P(U) + \text{constant } \cos\varphi_{PV} = 0.925$ over excited inverter regulation: Frequency and voltage in transition from grid to island mode. Transition 1 above, transition 2 middle, transition 3 below

Frequency behaviour during the transition shows, that ROCOF anti-islanding detection method would again be the most meaningful solution in order to make the NDZ narrower.

5.3.3 $Q(U)$ inverter regulation

Figure 5.16 depicts three chosen points within NDZ, where behaviour of frequency and voltage was recorded. Transition 1 was recorded in the right point on the figure, transition 2 in the middle point and transition 3 in the left point.

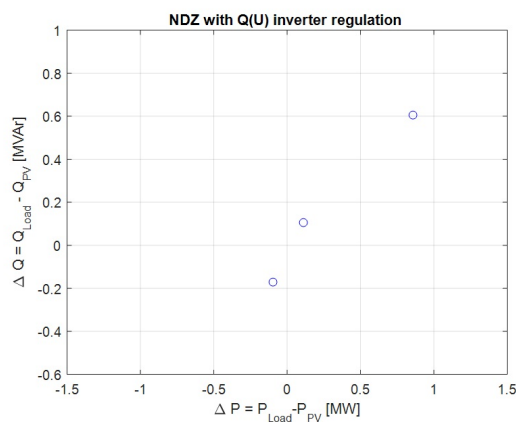


Figure 5.16: $Q(U)$ inverter regulation: Transition points. Transition 1 right, transition 2 middle, transition 3 left

Chosen transitions can be seen in Figure 5.17. From transitions of voltage, it can be concluded that regulation of reactive power in dependency to voltage also results in fluctuation of voltage (transition 2 and 3). Actually, fluctuation of reactive power has even bigger influence on voltage than fluctuation of active power. Oscillations of voltage are bigger than in previous cases, where only active power regulation was introduced. In transition 1, there is only small oscillation of voltage, because voltage is so low, that reactive power is constant and influences voltage only at the start of transition period. Voltage is after that stabilized at almost constant value.

Jumps of frequency at the start of transition periods from grid to island mode can again be clearly seen. Therefore, ROCOF would again be most suitable additional anti-islanding detection method in order to make NDZ a bit narrower.

5 Results and analysis

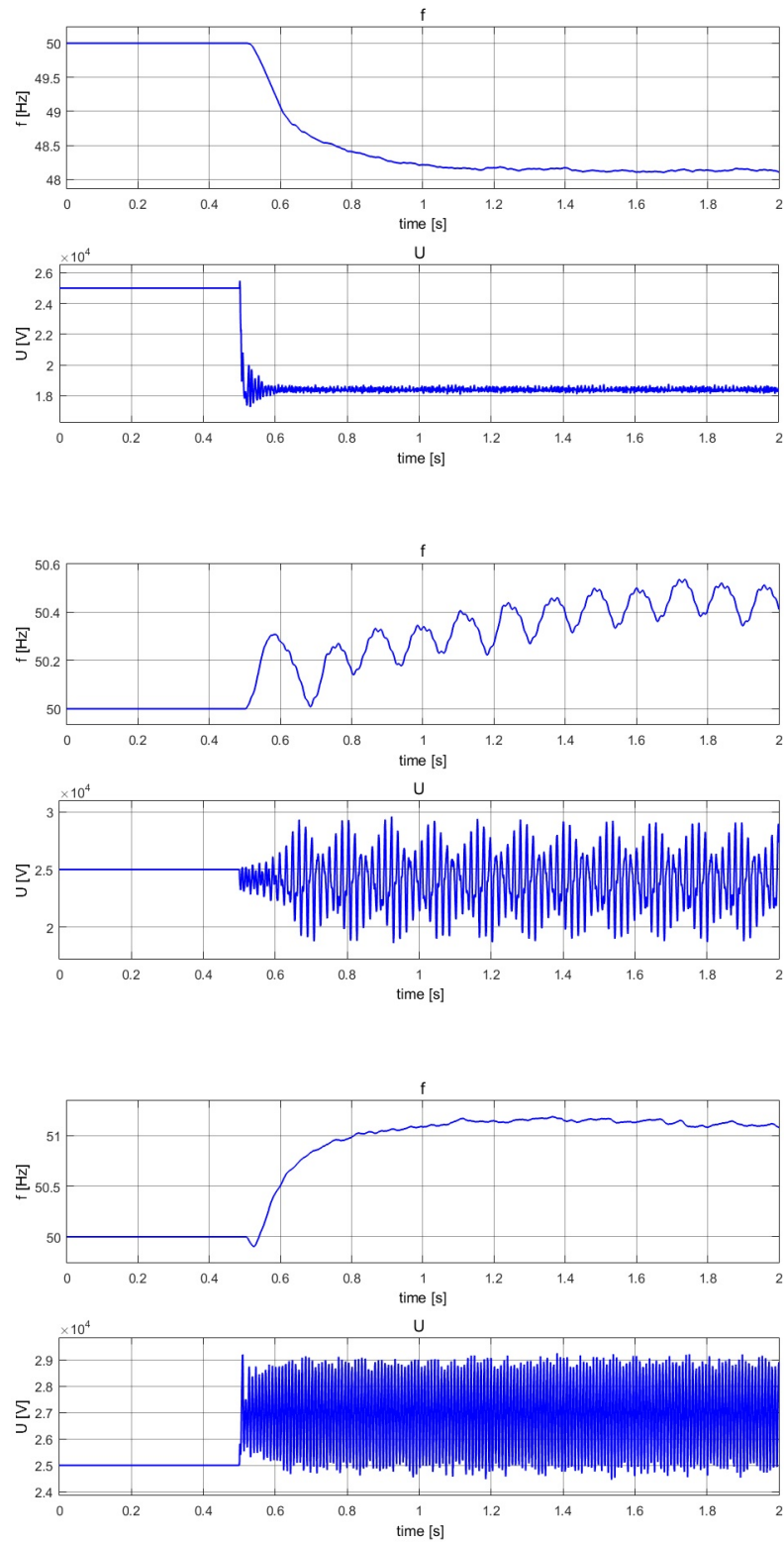


Figure 5.17: $Q(U)$ inverter regulation: Frequency and voltage in transition from grid to island mode. Transition 1 above, transition 2 middle, transition 3 below

5.3.4 $\cos\varphi(U)$ inverter regulation

Figure 5.18 depicts three chosen points within NDZ, where behaviour of frequency and voltage was recorded. Transition 1 was recorded in the right point on the figure, transition 2 in the middle point and transition 3 in the left point.

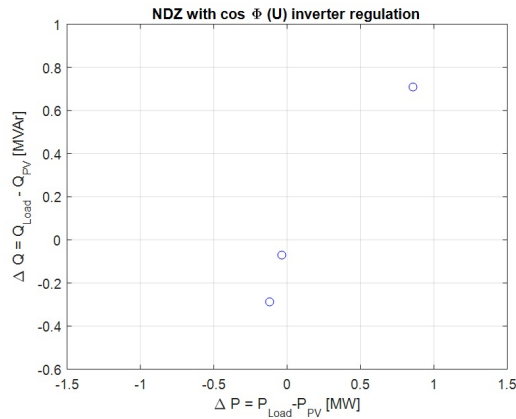


Figure 5.18: $\cos\varphi(U)$ inverter regulation: Transition points. Transition 1 right, transition 2 middle, transition 3 left

Chosen transitions can be seen in Figure 5.19. Graphs with $\cos\varphi(U)$ inverter regulation are very similar to the ones with $Q(U)$ inverter regulation. Voltage fluctuation is now result of reactive and active power regulation. In transition 1, there is only small oscillation of voltage, because voltage is so low, that reactive and active power are constant and influence voltage only at the start of transition period. Voltage is after that stabilized at almost constant value. The only surprise is frequency behaviour in transition 3, because the main jump of frequency happens at approximately 1.3s, which is unexpected, because all other jumps were recorded at 0.5 s. The reason for late jump is unclear.

5.4 Simulink model's efficiency

The reason for testing Simulink model's efficiency was the duration of simulation in real time. Working on computer with 0.80 GHz processor and 8 GB of RAM, the 2 s computer simulation time took 270s in real time. Knowing, that the space sweep for each of inverter regulations was done for at least 1500 points, it is clear why improving model's efficiency

5 Results and analysis

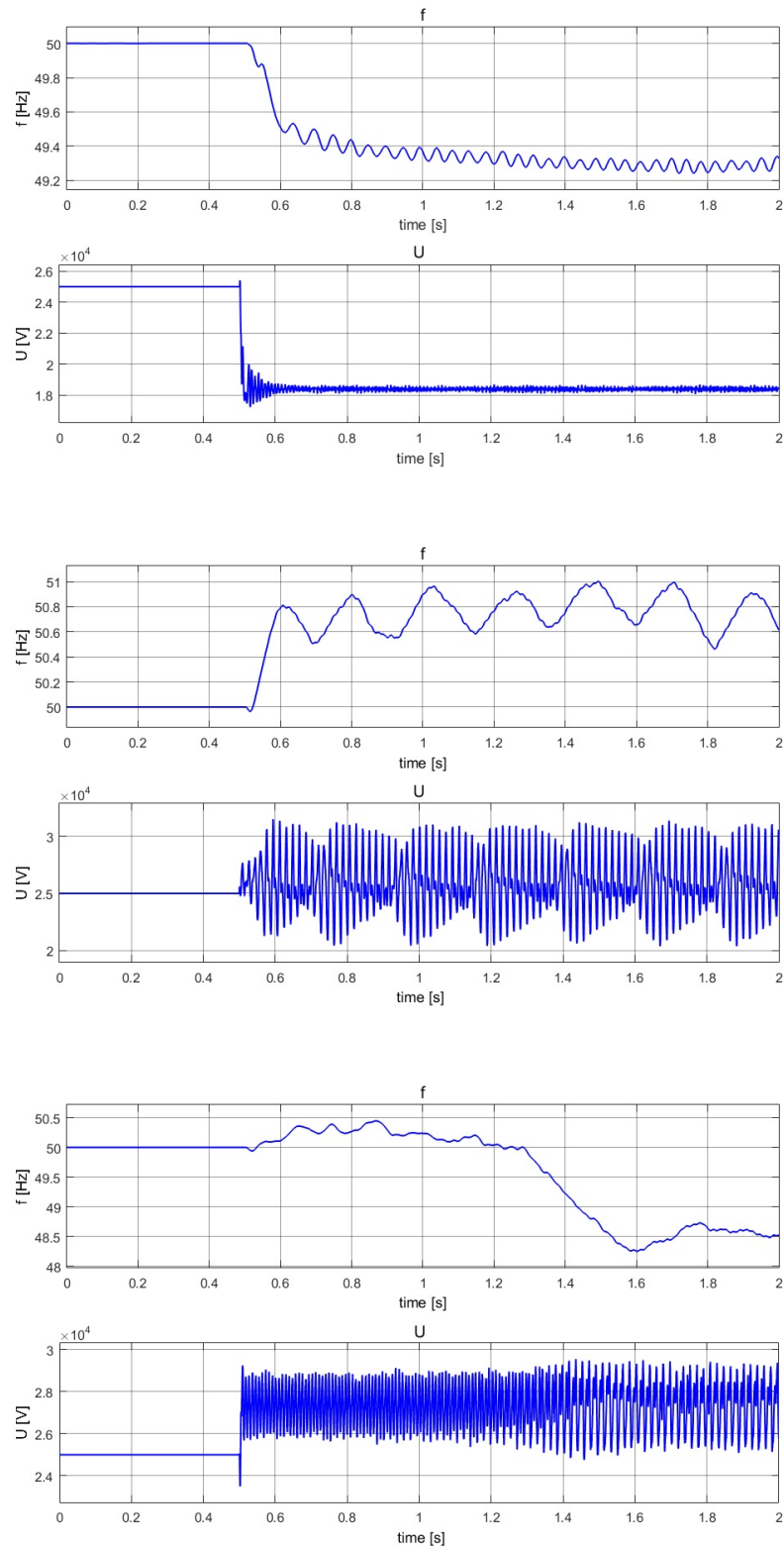


Figure 5.19: $\cos\varphi(U)$ inverter regulation: Frequency and voltage in transition from grid to island mode. Transition 1 above, transition 2 middle, transition 3 below

was researched.

Simulink profile report was used in order to get a better inside into the reasons, that could be slowing the model down. Built in functions, that were added for each of the inverter regulations took approximately 15 % of the time, but the biggest time consumer were simulation phase and major outputs of the model. Further research was done with studying of the simulation model with [17], because one of the existing Simulink models was used as a base for this thesis.

Based on the latter research, it was found out that changing of the sample time for pulse generator of boost and VSC controllers is by far the most effective way to reduce the simulation time. Bigger sample times however reduce the resolution of pulse-width-modulation waveforms of voltage. The original setting was sample time of 1 μs . Different bigger sample times were tested in order to find the best combination of time and resolution. As an example, NDZ with $P(U)$ inverter regulation and 10 μs sample time for pulse generator of boost and VSC controller can be looked at in Figure 5.20. Simulation with latter parameters took only 40s in real time. Time savings can however not replace the precision. NDZ in the Figure 5.20 is shifted downwards and much broader than NDZ with 1 μs sample time. Further examples were tried with sample times between 1 μs and 10 μs , but the conclusion was, that original setting with 1 μs sample time is optimal for the purposes of this thesis, where the precision of the acquired NDZ has the essential meaning.

5.5 Further research of $Q(U)$ inverter regulation

$Q(U)$ inverter regulation was chosen for further research among observed regulations due to several reasons. It is the most economically intriguing, because it does not regulate the active power, which means that economic yield of this inverter regulation is maximized. This regulation can also help with grid stabilization, because it can offer reactive power support to the grid, which could be useful for Volt Var Control. Possible application was researched in [26]. Sizes of simulated NDZs in the previous sections of this Chapter also show superiority of $Q(U)$ inverter regulation in comparison to other regulations. More specifically, NDZ with $Q(U)$ regulation is smaller than NDZs with $P(U)$ inverter regulation. Only NDZ with $\cos\varphi(U)$ inverter regulation is comparable in size, but is not that interesting, because its economic yield is not maximized.

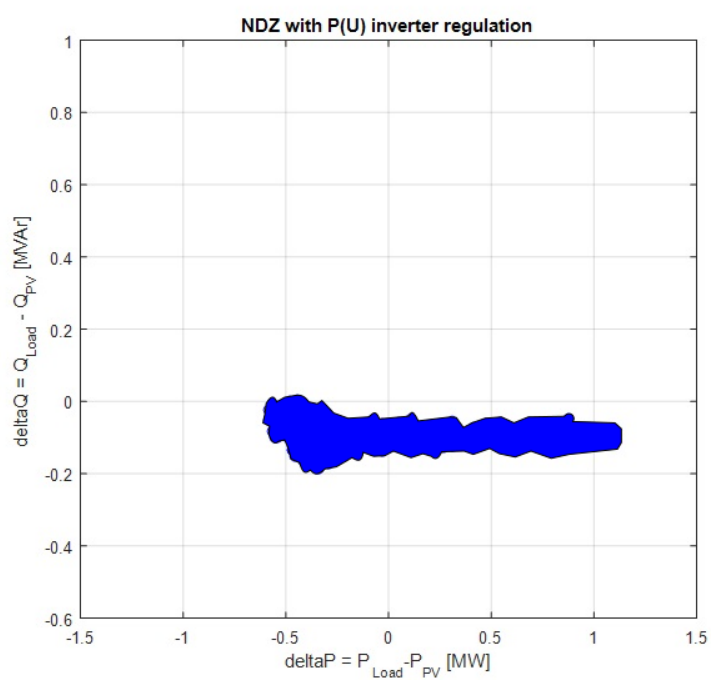


Figure 5.20: NDZ with $P(U)$ inverter regulation, sample time for pulse generator of boost and VSC controller: 10 μ s

This section offers research on combination of $Q(U)$ and $P(f)$ inverter regulations and additional introduction of ROCOF anti-islanding method to Simulink model in order to see its influence on NDZ area.

5.5.1 $Q(U)$ inverter regulation with ROCOF

ROCOF anti-islanding protection method was added to Simulink model in order to confirm or reject the conclusions from section 5.3. ROCOF should according to those conclusions have an influence on frequency protection borders of the NDZ. More specifically, it should make the NDZ narrower.

Paper [27] offered block diagram for rate of change of frequency implementation, Figure 5.21.

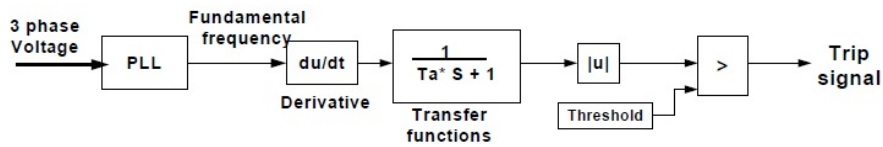


Figure 5.21: ROCOF block diagram, adopted from [27]

Block diagram from [27] was adjusted for the purposes of this thesis and can be seen in Figure 5.22. Since Simulink model used in this thesis is discrete time system model and sampling time is $T_s = 0.0001\text{s}$, Discrete Derivative block was used for sampling derivatives of frequency. Signal from Discrete Derivative block was then summed over 5000 sampling periods. This number was chosen based on observation of transitions from grid to island mode in section 5.3. The finding was, that the biggest jump was expected in time period from 0.5 s to 1 s. Pulse Generator resets Cumulative Sum block each 0.5 s. If change of frequency over this time exceeds 1 Hz or -1 Hz, then ROCOF protection detects the islanding.

Use of the described approach for ROCOF was used for this thesis, because certain characteristics of the model were taken into account. It should however be taken with caution and adjusted, if used for any other model.

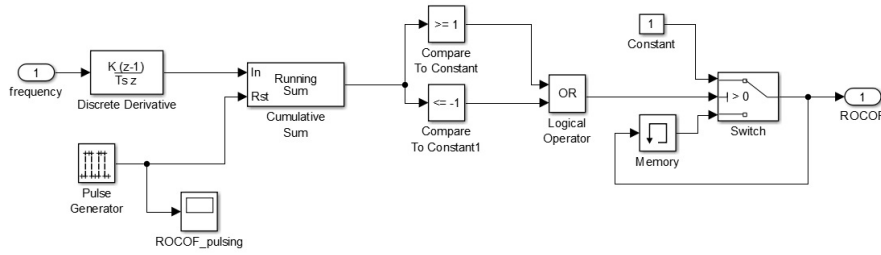


Figure 5.22: ROCOF block diagram from thesis's Simulink model

Figure 5.23 offers comparison of NDZs with $Q(U)$ inverter regulation with and without ROCOF anti-islanding protection method. Area on the right, where ROCOF was included, is as expected, noticeably narrower in comparison to NDZ on the left. Rate of change of frequency has influence only on frequency protection borders, which was anticipated.

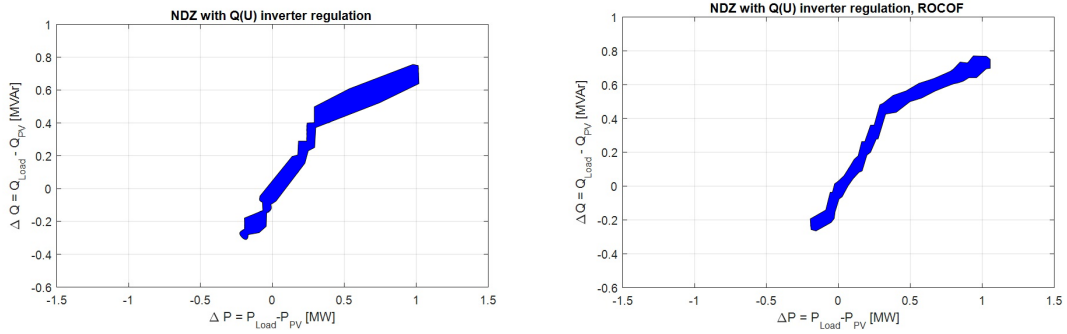


Figure 5.23: $Q(U)$ inverter regulation: left - without ROCOF, right - with ROCOF

5.5.2 $Q(U)$ and $P(f)$ inverter regulation

Additional $P(f)$ inverter regulation was chosen for analysis in combination with $Q(U)$, because of dispersed generation problem in continental Europe, described at the start of Chapter 3. This regulation predicts reduction of active power output of inverter, once certain frequency threshold is exceeded. The regulation's statics from TOR, [9] is depicted in Figure 5.24. The threshold value is at 50.2 Hz. Once frequency is above this value, momentary active power output is reduced for 40% per each Hertz. NDZ with combination of $Q(U)$ and $P(f)$ inverter regulations is expected to be bigger in width, because OFP

border is expected to be moved further up along the y axes.

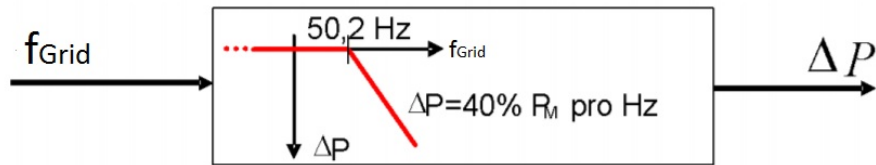


Figure 5.24: Statics for $P(f)$ inverter regulation, adapted on basis [9]

Figure 5.25 offers simulated NDZ with $Q(U)$ and $P(f)$ inverter regulation. As expected, the area is much wider than by the NDZ with only $Q(U)$ inverter regulation (Figure 5.8 on the right). UFP border (border below) is practically the same, OFP border (border above) is however moved up along the y axes. Shift of OFP border can be explained with understanding of $P(f)$ inverter regulation. The regulation reduces active power once certain frequency is exceeded and with that works towards stabilizing of the island. Another observation is, that $P(f)$ inverter regulation has much bigger influence on OFP border in the area closer to UVP border. So, the lower the voltage, the wider the NDZ area.

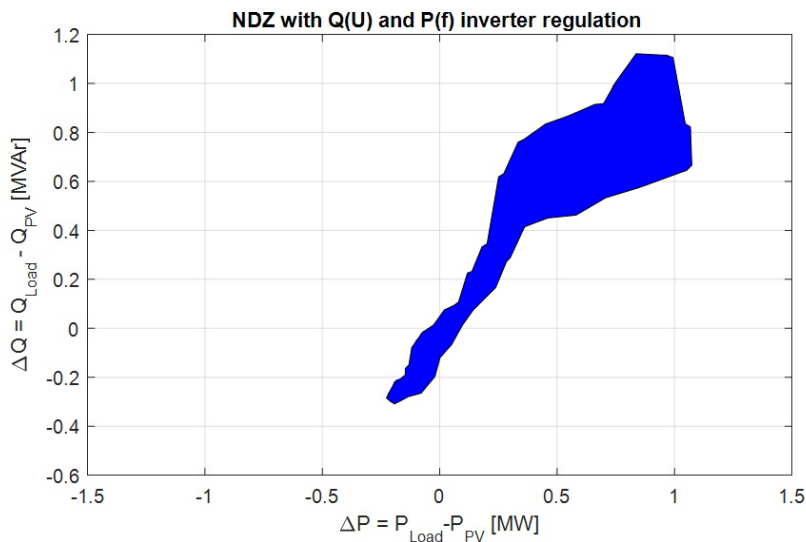


Figure 5.25: Simulated NDZ with $Q(U)$ and $P(f)$ inverter regulation, adapted with Inkscape

5.5.3 $Q(U)$ and $P(f)$ inverter regulation with ROCOF

Figure 5.26 offers comparison of NDZs with $Q(U)$ and $P(f)$ inverter regulation with and without ROCOF anti-islanding protection method. The effect of ROCOF is again clearly seen. NDZ on the right is much narrower in width, the length of the zone however remains practically the same.

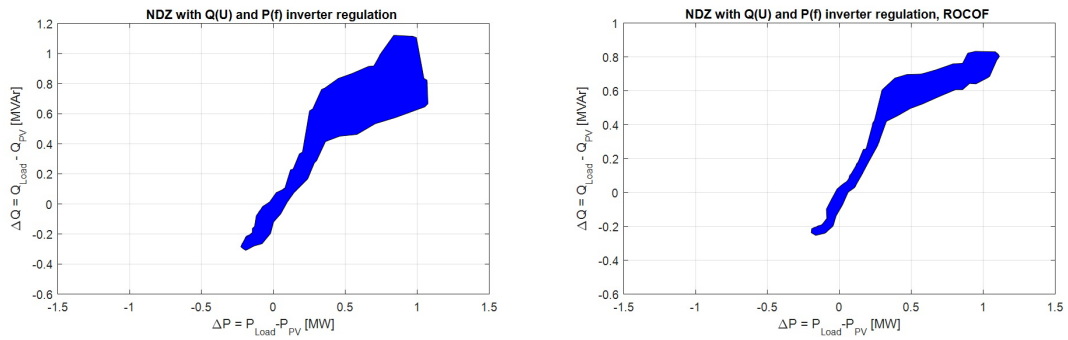


Figure 5.26: $Q(U)$ and $P(f)$ inverter regulation: left - without ROCOF, right - with ROCOF

6 Conclusion and future work

Theoretical research of the islanding problem in collaboration with growing amount of DER in continental Europe showed, that finding an appropriate and cost effective anti-islanding protection method is a very important task for reliable operation of future smart power grid. The fact, that big frequency jumps are mostly influenced by electricity markets, shows, that power grid is not any more mainly focused on reliability and security but also on ecology and especially economy.

Applied Matlab Simulink model, which was used for obtaining simulated NDZs, offered certain advantages and disadvantages. Basis for the model was taken from Simscape Power Systems in Simulink, which saved a lot of time. Base model also offered a lot of additional functions (like irradiation and temperature of the PV modules) and they could be potentially interesting for observation, but were not meaningful for the scope of this thesis. In conclusion, model offered more than satisfactory results, but was also pre-dimensioned, given the real world simulation time, that was needed for each simulation.

The comparison of analytical and simulated NDZs showed, that analytical approach used in the thesis was good. Except for the “break areas” of the NDZs, where inverter regulations change their influence on the inverter output and for the fact, that dynamic behaviour of frequency and voltage after split from the grid cannot be anticipated, the borders found with analytical calculations were similar to the ones, found with simulations.

Results (NDZs acquired with OVP/UVP and OFP/UFP protection methods and transitions from grid to island mode) showed that $Q(U)$ inverter regulation is the best among researched options for protection against islanding in terms of technical and economical reasons. Its NDZ area was the smallest, which means, that islanding is least likely to

6 Conclusion and future work

happen, when this inverter regulation is in place. Further research on this inverter regulation showed, that ROCOF anti-islanding method noticeably reduces NDZ area. ROCOF effect is especially clearly seen, when used with $Q(U)$ and $P(f)$ inverter regulation. Latter regulation was introduced, because addition of $P(f)$ to $Q(U)$ inverter regulation offers additional security for European power grid and could offer reasonable compromise in both, technical and economical sense.

Based on the thesis findings, following research areas remain open:

- Further research of anti-islanding protection methods (passive, active and remote)
- Further research of inverter regulations
- Improvement or making of new Matlab Simulink model
- Further research of threshold values of anti-islanding methods (maybe real world application)

List of Figures

1.1	Mandatory national targets for all EU member states, adopted from [2] . . .	2
1.2	Basic configuration for presentation of islanding, adopted from [4]	3
2.1	Statics for $\cos\varphi(P)$, adapted on basis [6]	9
2.2	NDZ, adapted on basis [6]	9
2.3	NDZ: Only active power output (above), Active and reactive power output with constant $\cos\varphi$ (middle), Active and reactive power output with constant $\cos\varphi$ and active power reduction by over-frequency (below), adopted from [6]	12
3.1	Reactive power areas, adapted on basis [9]	18
3.2	Q(U) curve for LV grids, adopted from [9]	20
3.3	$\cos\varphi(U)$ curve, adopted from [10]	21
3.4	P(U) curve, adopted from [9]	21
3.5	Feeder configuration showing power flows, adopted from [11]	24
3.6	Operation of the phase jump detection method, adopted from [11]	25
3.7	A BRP is only constrained by the energy exchange per PTU, adopted from [14]	27
3.8	Monthly and yearly averages of frequency deviations in the period from March 2008 to February 2009, adopted from [14]	28
4.1	Schematic representation of Simulink model, made with SmartDraw2017 . . .	31
4.2	Characteristic PV Array power curve, adopted from [19]	33
4.3	OVP/UVP and OFP/UFP protection in MATLAB Simulink model	35
4.4	Plotting of NDZ, adopted from [22]	36
4.5	Gathering of NDZ in MATLAB Simulink model	36

List of Figures

4.6	Inverter regulations	37
4.7	$P(U)$ inverter regulation statics	40
4.8	Analytical NDZ with $P(U)$ inverter regulation	42
4.9	Analytical NDZ with $P(U) + \text{constant } \cos\varphi_{PV} = 0.925$ over excited in- verter regulation	44
4.10	$Q(U)$ inverter regulation statics	46
4.11	Analytical NDZ with $Q(U)$ inverter regulation	47
4.12	$\cos\varphi(U)$ inverter regulation statics	49
4.13	Analytical NDZ with $\cos\varphi(U)$ inverter regulation	50
4.14	Explanation of green filled areas from Figure 4.13	51
5.1	NDZ with only active power output - Standard Zone	56
5.2	NDZ with only active power output - Standard Zone, adapted with Inkscape	57
5.3	Comparison of analytical and simulated NDZs with only active power out- put - Standard Zone	58
5.4	$P(U)$ inverter regulation: left - NDZ space sweep, right - NDZ adapted with Inkscape	59
5.5	Comparison of analytical and simulated NDZs with $P(U)$ inverter regulation	60
5.6	$P(U) + \text{constant } \cos\varphi_{PV} = 0.925$ inverter regulation: left - NDZ space sweep, right - NDZ adapted with Inkscape	62
5.7	Comparison of analytical and simulated NDZs with $P(U) + \text{constant } \cos\varphi_{PV} =$ 0.925 inverter regulation	63
5.8	$Q(U)$ inverter regulation: left - NDZ space sweep, right - NDZ adapted with Inkscape	63
5.9	Comparison of analytical and simulated NDZs with $Q(U)$ inverter regulation	64
5.10	$\cos\varphi(U)$ inverter regulation: left - NDZ space sweep, right - NDZ adapted with Inkscape	65
5.11	Comparison of analytical and simulated NDZs with $\cos\varphi(U)$ inverter regu- lation	66
5.12	$P(U)$ inverter regulation: Transition points. Transition 1 right, transition 2 middle, transition 3 left	67

5.13	$P(U)$ inverter regulation: Frequency and voltage in transition from grid to island mode. Transition 1 above, transition 2 middle, transition 3 below . . .	68
5.14	$P(U) + \text{constant } \cos\varphi = 0.925 \text{ over excited}$ inverter regulation: Transition points. Transition 1 right, transition 2 middle, transition 3 left	69
5.15	$P(U) + \text{constant } \cos\varphi_{PV} = 0.925 \text{ overexcited}$ inverter regulation: Frequency and voltage in transition from grid to island mode. Transition 1 above, transition 2 middle, transition 3 below	70
5.16	$Q(U)$ inverter regulation: Transition points. Transition 1 right, transition 2 middle, transition 3 left	71
5.17	$Q(U)$ inverter regulation: Frequency and voltage in transition from grid to island mode. Transition 1 above, transition 2 middle, transition 3 below . . .	72
5.18	$\cos\varphi(U)$ inverter regulation: Transition points. Transition 1 right, transition 2 middle, transition 3 left	73
5.19	$\cos\varphi(U)$ inverter regulation: Frequency and voltage in transition from grid to island mode. Transition 1 above, transition 2 middle, transition 3 below	74
5.20	NDZ with $P(U)$ inverter regulation, sample time for pulse generator of boost and VSC controller: $10 \mu\text{s}$	76
5.21	ROCOF block diagram, adopted from [27]	77
5.22	ROCOF block diagram from thesis's Simulink model	78
5.23	$Q(U)$ inverter regulation: left - without ROCOF, right - with ROCOF . . .	78
5.24	Statics for $P(f)$ inverter regulation, adapted on basis [9]	79
5.25	Simulated NDZ with $Q(U)$ and $P(f)$ inverter regulation, adapted with Inkscape	79
5.26	$Q(U)$ and $P(f)$ inverter regulation: left - without ROCOF, right - with ROCOF	80

List of Tables

2.1	Protection set points for inverters on LV grid, adapted on basis [6]	8
2.2	Overview of advantages and disadvantages of anti-islanding protection methods, adapted on basis [6]	10
3.1	Reactive power areas for medium voltage grid, adopted from [9]	17
4.1	Protection set points for inverters on MV grid, adopted from [9]	34
4.2	RLC load values in null point	39
4.3	Voltage set points for $P(U)$ regulation	40
4.4	NDZ borders for $P(U)$ inverter regulation	43
4.5	NDZ borders for $P(U) + constant \cos\varphi_{PV} = 0.925$ over excited inverter regulation	45
4.6	Voltage set points for $Q(U)$ regulation	45
4.7	NDZ borders for $Q(U)$ inverter regulation, rectangle in the middle	46
4.8	NDZ borders for $Q(U)$ inverter regulation, shape on the left of the rectangle	47
4.9	NDZ borders for $Q(U)$ inverter regulation, shape on the right of the rectangle	48
4.10	NDZ borders for $Q(U)$ inverter regulation, shape on the far right	48
4.11	Voltage set points for $\cos\varphi(U)$ regulation	49
4.12	NDZ borders for $\cos\varphi(U)$ inverter regulation, shape on the left of the rectangle	52
4.13	NDZ borders for $\cos\varphi(U)$ inverter regulation, shape on the right of the rectangle	52
4.14	NDZ borders for $\cos\varphi(U)$ inverter regulation, shape on the far right	52
5.1	Parameters for space sweep of standard zone	57
5.2	Parameters for space sweep of $P(U)$ inverter regulation	59
5.3	Parameters for space sweep of $P(U) + constant \cos\varphi_{PV} = 0.925$ over excited inverter regulation	61
5.4	Parameters for space sweep of $Q(U)$ inverter regulation	63
5.5	Parameters for space sweep of $\cos\varphi(U)$ inverter regulation	65

Bibliography

- [1] H.B. Puttgen, P.R. MacGregor, and F.C. Lambert. Distributed generation: Semantic hype or the dawn of a new era? *IEEE Power and Energy Magazine*, 99:22 – 29, 2003. 1
- [2] Dörte Fouquet. Policy instruments for renewable energy – from a european perspective. *Renewable energy*, 49:15 – 18, 2013. 1, 2, 83
- [3] R.W. Uluski. Vvc in the smart grid era. 2010. 1
- [4] Ku Nurul Edhura Ku Ahmad, Jeyraj Selvaraj, and Nasrudin Abd Rahim. A review of the islanding detection methods in grid-connected pv inverters. *Renewable and Sustainable Energy Reviews*, 21:756–766, 2013. 2, 3, 4, 23, 83
- [5] A.R.D. Fazio, M. Russo, and S.A. Valeri. A new protection system for islanding detection in lv distribution systems. *Energies 2015*, 8:3775 – 3793, 2013. 3
- [6] David Springer. Analyse von verfahren zur detektion ungewollter elektrischer inselnetze. Master’s thesis, TU Wien, 2016. 4, 7, 8, 9, 10, 11, 12, 16, 35, 83, 86
- [7] EuropeanCommission. Dispersed generation impact on ce region security. 2013. 15, 19
- [8] Miha Flegar and Gašper Škarja. Preprečevanje otočnega obratovanja omrežnih fotonapetostnih sistemov v luči standarda din vde 0126-1-1. *Konferenca slovenskih elektroenergetikov*, pages 1 – 4, 2007. 15
- [9] Austria Energie Control. Technische und organisatorische regeln für betreiber und benutzer von netzen. 2016. 16, 17, 18, 20, 21, 34, 40, 45, 48, 78, 79, 83, 85, 86
- [10] Radauer Markus. Parametrierung von pv-wechselrichtern. 2015. 20, 21, 48, 83

Bibliography

- [11] Ward Bower and Michael Ropp. Evaluation of islanding detection methods for utility-interactive inverters in photovoltaic systems. 2002. 23, 24, 25, 83
- [12] A. Y. Hatata, El-h. Abd-Raboh, and E. Sedhom. A review of anti-islanding protection methods for renewable distributed generation systems. *Journal of Electrical Engineering*, pages 1 – 12, 2015. 23, 26, 29
- [13] Francesco De Mango, Marco Liserre, Antonio Dell’Aquila, and Alberto Pigazo. Overview of anti-islanding algorithms for pv systems part i: Passive methods. *IEEE Conference Publications*, pages 1878 – 1883, 2006. 23
- [14] Jasper Frunt, Ioannis Lampropoulos, and Wil L. Kling. The impact of electricity market design on periodic network frequency excursions. 2011. 27, 28, 83
- [15] CommissionForEnergyRegulation. Review of tso and generator submissions. 2013. 28
- [16] Ontrei Raipala, Anssi Makinen, and Sami Repo. An anti-islanding protection method based on reactive power injection and rocof. *IEEE Transactions on power delivery*, 32:401 – 410, 2017. 28
- [17] Mathworks. <https://de.mathworks.com/help/physmod/sps/examples/detailed-model-of-a-100-kw-grid-connected-pv-array.html>. Accessed: 2017-04-17. 31, 33, 75
- [18] Jitendra Kasera, Vinod Kumar, R.R. Dr. Joshi, and Jai Kumar Maherchandani. Design of grid connected photovoltaic system employing incremental conductance mppt algorithm. *Journal of Electrical Engineering*, pages 1 – 6, 2012. 32
- [19] Trishan ESRAM and Patrick L. Chapman. Comparison of photovoltaic array maximum power point tracking techniques. *IEEE Transactions on energy conversion*, 22:439 – 449, 2007. 32, 33, 83
- [20] Concettine Buccella, Carlo Cecati, Hamed Letafat, and Kaveh Razi. A grid-connected pv system with llc resonant dc-dc converter. *IEEE*, pages 777 – 782, 2013. 33
- [21] Wolfgang Gawlik. *Energieversorgung*. Studium und Praxis. TU Wien, 2014. 33

- [22] Michael E. Ropp, Miroslav Begovic, Ajeet Rohatgi, Gregory A. Kern, R. H. Bonn, and S. Gonzales. Determining the relative effectiveness of islanding detection methods using phase criteria and nondetection zones. *IEEE Transactions on energy conversion*, 15:290 – 296, 2000. 35, 36, 83
- [23] Ye Zhihong, Amol Kolwalkar, Rhei Walling, Yu Zhang, and Du Pengwei. Evaluation of anti-islanding schemes based on nondetection zone concept. *IEEE Transactions on power electronics*, 19:1171 – 1176, 2004. 35
- [24] Ravi Raj and Mande Praveen. Survey of islanding detection techniques for grid connected photovoltaic inverters. *International Journal of Computer Science and Network*, 6:14 – 23, 2017. 35
- [25] EuropeanComission. Commission regulation (eu) 2016/1388 of 17 august 2016 establishing a network code on demand connection. 2016. 39
- [26] Pedran Jahangiri and Aliprantis C. Dionysios. Distributed volt/var control by pv inverters. *IEEE Transactions on power systems*, 28:3429 – 3439, 2013. 75
- [27] X. Ding and A. Crossley, P. Islanding detection for distributed generation. 2005. 77, 85

Eidesstattliche Erklärung

Hiermit erkläre ich, dass die vorliegende Arbeit gemäß dem Code of Conduct – Regeln zur Sicherung guter wissenschaftlicher Praxis (in der aktuellen Fassung des jeweiligen Mitteilungsblattes der TU Wien), insbesondere ohne unzulässige Hilfe Dritter und ohne Benutzung anderer als der angegebenen Hilfsmittel, angefertigt wurde. Die aus anderen Quellen direkt oder indirekt übernommenen Daten und Konzepte sind unter Angabe der Quelle gekennzeichnet. Die Arbeit wurde bisher weder im In- noch im Ausland in gleicher oder in ähnlicher Form in anderen Prüfungsverfahren vorgelegt.

Wien, Thursday 21st September, 2017

Klemen Peter Kosovinc

